REFERENCES

[1] Roser, M., Ritchie, H., Cancer. *Our World in Data* 2015.

[2] Worldwide cancer data | World Cancer Research Fund International. *WCRF International* (2023).

[3] Phi, L.T.H., Sari, I.N., Yang, Y.-G., Lee, S.-H., et al., Cancer Stem Cells (CSCs) in Drug Resistance and their Therapeutic Implications in Cancer Treatment. *Stem Cells International* 2018, *2018*, e5416923.

[4] Nanda, S., Moore, H., Lenhart, S., Optimal control of treatment in a mathematical model of chronic myelogenous leukemia. *Mathematical Biosciences* 2007, *210*, 143–156.

[5] Wheeler, C.J., Das, A., Liu, G., Yu, J.S., et al., Clinical responsiveness of glioblastoma multiforme to chemotherapy after vaccination. *Clin Cancer Res* 2004, *10*, 5316–5326.

[6] Fenstermaker, R.A., Ciesielski, M.J., Immunotherapeutic strategies for malignant glioma. *Cancer Control* 2004, *11*, 181–191.

[7] Everson, T.C., Spontaneous regression of cancer. *Prog Clin Cancer* 1967, *3*, 79–95.

[8] Hoption Cann, S.A., van Netten, J.P., van Netten, C., Glover, D.W., Spontaneous regression: a hidden treasure buried in time. *Medical Hypotheses* 2002, *58*, 115–119.

[9] Hoption Cann, S.A., van Netten, J.P., van Netten, C., Dr William Coley and tumour regression: a place in history or in the future. *Postgraduate Medical Journal* 2003, *79*, 672–680.

[10] Zahl, P.-H., Gøtzsche, P.C., Mæhlen, J., Natural history of breast cancers detected in the Swedish mammography screening programme: a cohort study. *The Lancet Oncology* 2011, *12*, 1118–1124.

[11] Fryback, D.G., Stout, N.K., Rosenberg, M.A., Trentham-Dietz, A., et al., Chapter 7: The Wisconsin Breast Cancer Epidemiology Simulation Model. *JNCI Monographs* 2006, *2006*, 37–47.

[12] sponteneous regression of cancer or sponteneous remission of cancer - Search Results - PubMed. (2023).

[13] Kaiser, H.E., Biological viewpoints of neoplastic regression. *In Vivo* 1994, *8*, 155–165.

[14] Perry, M.C., Doll, D.C., Freter, C.E. (Eds.), Chemotherapy source book, 5th ed, Wolters Kluwer/Lippincott Williams & Wilkins, Philadelphia 2012.

[15] Dutta, M.D., Roy, P.K., Frank H. George Research Award winning paper Cancer self-remission and tumour instability – a cybernetic analysis Towards a fresh paradigm for cancer treatment. *Kybernetes* 2000, *29*, 896–927.

[16] Schmidt, W., Eisen, M.: Mathematical Models in Cell Biology and Cancer Chemotherapy. Lecture Notes in Biomathematics, vol. 30. Springer-Verlag, Berlin-Heidelberg-New York 1979. IX, 431 S., 70 Abb., 17 Tab., DM 39,—. *Biometrical Journal* 1981, *23*, 519–520.

[17] Coldman, A.J., Goldie, J.H., A stochastic model for the origin and treatment of tumours containing drug-resistant cells. *Bulletin of Mathematical Biology* 1986, *48*, 279–292.

[18] Skipper, H.E., On mathematical modeling of critical variables in cancer treatment (goals: better understanding of the past and better planning in the future). *Bull Math Biol* 1986, *48*, 253–278.

[19] Bellomo, N., Preziosi, L., Modelling and mathematical problems related to tumour evolution and its interaction with the immune system. *Mathematical and Computer Modelling* 2000, *32*, 413–452.

[20] Sakode, C.M., Padhi, R., Kapoor, S., Rallabandi, V.P.S., et al., Multimodal therapy for complete regression of malignant melanoma using constrained nonlinear optimal dynamic inversion. *Biomedical Signal Processing and Control* 2014, *13*, 198–211.

[21] Kondo, N., Takahashi, A., Ono, K., Ohnishi, T., DNA Damage Induced by Alkylating Agents and Repair Pathways. *Journal of Nucleic Acids* 2010, *2010*, e543531.

[22] Friedberg, E.C., McDaniel, L.D., Schultz, R.A., The role of endogenous and exogenous DNA damage and mutagenesis. *Current Opinion in Genetics & Development* 2004, *14*, 5–10.

[23] Lodish, H.F., Berk, A., Kaiser, C., Krieger, M., et al., Molecular cell biology, W.H. Freeman, New York 2008.

[24] Dunn, G.P., Bruce, A.T., Ikeda, H., Old, L.J., et al., Cancer immunoediting: from immunosurveillance to tumour escape. *Nat Immunol* 2002, *3*, 991–998.

[25] Dunn, G.P., Old, L.J., Schreiber, R.D., The immunobiology of cancer immunosurveillance and immunoediting. *Immunity* 2004, *21*, 137–148.

[26] Mg, E., Rc, T., R, A., Ak, S., et al., Intracranial paracrine interleukin-2 therapy stimulates prolonged antitumour immunity that extends outside the central nervous system. *Journal of Immunotherapy (Hagerstown, Md. : 1997)* 2000, *23*.

[27] de Pillis, L.G., Gu, W., Radunskaya, A.E., Mixed immunotherapy and chemotherapy of tumours: modeling, applications and biological interpretations. *Journal of Theoretical Biology* 2006, *238*, 841–862.

[28] Kuznetsov, V.A., Makalkin, I.A., Taylor, M.A., Perelson, A.S., Nonlinear dynamics of immunogenic tumours: Parameter estimation and global bifurcation analysis. *Bulletin of Mathematical Biology* 1994, *56*, 295–321.

[29] Kirschner, D., Panetta, J.C., Modeling immunotherapy of the tumour-immune interaction. *J Math Biol* 1998, *37*, 235–252.

[30] de Pillis, L.G., Radunskaya, A.E., Wiseman, C.L., A Validated Mathematical Model of Cell-Mediated Immune Response to Tumour Growth. *Cancer Research* 2005, *65*, 7950–7958.

[31] Cancer Facts & Figures 2022| American Cancer Society,(2023).

[32] Sumner, W.C., Spontaneous regression of melanoma. Report of a case. *Cancer* 1953, *6*, 1040–1043.

[33] Ceballos, P.I., Barnhill, R.L., Spontaneous regression of cutaneous tumours. *Adv Dermatol* 1993, *8*, 229–261; discussion 262.

[34] Blessing, K., McLaren, K.M., Histological regression in primary cutaneous melanoma: recognition, prevalence and significance. *Histopathology* 1992, *20*, 315–322.

[35] Ribero, S., Gualano, M.R., Osella-Abate, S., Scaioli, G., et al., Association of Histologic Regression in Primary Melanoma With Sentinel Lymph Node Status: A Systematic Review and Meta-analysis. *JAMA Dermatology* 2015, *151*, 1301–1307.

[36] Melanoma research gathers momentum. *Lancet* 2015, *385*, 2323.

[37] Rambow, F., Piton, G., Bouet, S., Leplat, J.-J., et al., Gene Expression Signature for Spontaneous Cancer Regression in Melanoma Pigs. *Neoplasia* 2008, *10*, 714-IN5.

[38] Daphu, I., Horn, S., Stieber, D., Varughese, J.K., et al., In Vitro Treatment of Melanoma Brain Metastasis by Simultaneously Targeting the MAPK and PI3K Signaling Pathways. *Int J Mol Sci* 2014, *15*, 8773–8794.

[39] Kunz, M., Vera, J., Modelling of Protein Kinase Signaling Pathways in Melanoma and Other Cancers. *Cancers (Basel)* 2019, *11*, 465.

[40] Palmieri, G., Capone, M., Ascierto, M.L., Gentilcore, G., et al., Main roads to melanoma. *J Transl Med* 2009, *7*, 86.

[41] Goel, V.K., Lazar, A.J.F., Warneke, C.L., Redston, M.S., et al., Examination of mutations in BRAF, NRAS, and PTEN in primary cutaneous melanoma. *J Invest Dermatol* 2006, *126*, 154–160.

[42] Rebocho, A.P., Marais, R., ARAF acts as a scaffold to stabilize BRAF:CRAF heterodimers. *Oncogene* 2013, *32*, 3207–3212.

[43] Davies, H., Bignell, G.R., Cox, C., Stephens, P., et al., Mutations of the BRAF gene in human cancer. *Nature* 2002, *417*, 949–954.

[44] Pollock, P.M., Harper, U.L., Hansen, K.S., Yudt, L.M., et al., High frequency of BRAF mutations in nevi. *Nat Genet* 2003, *33*, 19–20.

[45] Giehl, K., Oncogenic Ras in tumour progression and metastasis. *Biol Chem* 2005, *386*, 193–205.

[46] Arcaro, A., Guerreiro, A.S., The phosphoinositide 3-kinase pathway in human cancer: genetic alterations and therapeutic implications. *Curr Genomics* 2007, *8*, 271–306.

[47] Stark, M., Hayward, N., Genome-wide loss of heterozygosity and copy number analysis in melanoma using high-density single-nucleotide polymorphism arrays. *Cancer Res* 2007, *67*, 2632–2642.

[48] Stahl, J.M., Sharma, A., Cheung, M., Zimmerman, M., et al., Deregulated Akt3 activity promotes development of malignant melanoma. *Cancer Res* 2004, *64*, 7002–7010.

[49] Vladimirova, I.G., The Energetics of Regeneration Processes, in: *The Energetics of Regeneration Processes*, De Gruyter, 2019, pp. 243–256.

[50] Biktimirov, T.Z., Butov, A.A., Savinov, Yu.G., Optimal control of the moment of spontaneous tumour regression. *Autom Remote Control* 2005, *66*, 658–663.

[51] Roy, P.K., Kozma, R., Majumder, D.D., From neurocomputation to immunocomputation - a model and algorithm for fluctuation-induced instability and phase transition in biological systems. *IEEE Transactions on Evolutionary Computation* 2002, *6*, 292–305.

[52] Singh, S., Padhi, R., Automatic path planning and control design for autonomous landing of UAVs using dynamic inversion, in: *2009 American Control Conference*, 2009, pp. 2409–2414.

[53] H. Khalil, Nonlinear Systems, 2th edition, in Prentice-Hall, New Jersey, 1996.

[54] Hall, J.E., Guyton, A.C., Guyton and Hall textbook of medical physiology, 12th ed, Saunders/Elsevier, Philadelphia, Pa 2011.

[55] Del Monte, U., Does the cell number 10(9) still really fit one gram of tumour tissue? *Cell Cycle* 2009, *8*, 505–506.

[56] Calabresi, P., etc (Eds.), Medical Oncology: Basic Principles and Clinical Management of Cancer, 2nd edition, McGraw-Hill Professional, New York 1993.

[57] Diefenbach, A., Jensen, E.R., Jamieson, A.M., Raulet, D.H., Rae1 and H60 ligands of the NKG2D receptor stimulate tumour immunity. *Nature* 2001, *413*, 165–171.

[58] Dudley, M.E., Wunderlich, J.R., Robbins, P.F., Yang, J.C., et al., Cancer regression and autoimmunity in patients after clonal repopulation with antitumour lymphocytes. *Science* 2002, *298*, 850–854.

[59] Yates, A., Callard, R., Cell death and the maintenance of immunological memory. *Discrete and Continuous Dynamical Systems: Series B* 2001, *1*, 43–59.

[60] Lanzavecchia, A., Sallusto, F., Dynamics of T lymphocyte responses: intermediates, effectors, and memory cells. *Science* 2000, *290*, 92–97.

[61] Macintyre, E.A., Linch, D.C., Lymphocytosis: is it leukaemia and when to treat. *Postgraduate Medical Journal* 1988, *64*, 42–47.

[62] Jarosz, M., Hak, Ł., Więckiewicz, J., Balcerska, A., et al., Clinical immunology
NK cells in children with acute lymphoblastic leukemia and non-Hodgkin lymphoma after cessation of intensive chemotherapy. *Cent Eur J Immunol* 2009, *34*, 94–99.

[63] Berrington, J.E., Barge, D., Fenton, A.C., Cant, A.J., et al., Lymphocyte subsets in term and significantly preterm UK infants in the first year of life analysed by single platform flow cytometry. *Clin Exp Immunol* 2005, *140*, 289–292.

[64] Jawahar, S., Moody, C., Chan, M., Finberg, R., et al., Natural killer (NK) cell deficiency associated with an epitope-deficient Fc receptor type IIIA (CD16-II). *Clinical and Experimental Immunology* 1996, *103*, 408.

[65] Hicks, A.M., Riedlinger, G., Willingham, M.C., Alexander-Miller, M.A., et al., Transferable anticancer innate immunity in spontaneous regression/complete resistance mice. *Proc Natl Acad Sci U S A* 2006, *103*, 7753–7758.

[66] Foo, J., Michor, F., Evolution of resistance to anti-cancer therapy during general dosing schedules. *J Theor Biol* 2010, *263*, 179–188.

[67] Zotin, A.I., Thermodynamic Bases of Biological Processes: Physiological Reactions and Adaptations, Walter de Gruyter, 1990.

[68] Smith, K.A., Interleukin-2: inception, impact, and implications. *Science* 1988, *240*, 1169–1176.

[69] Gao, Q., Zhou, G., Lin, S.-J., Paus, R., et al., How chemotherapy and radiotherapy damage the tissue: Comparative biology lessons from feather and hair models. *Exp Dermatol* 2019, *28*, 413–418.

[70] Yarana, C., St. Clair, D.K., Chemotherapy-Induced Tissue Injury: An Insight into the Role of Extracellular Vesicles-Mediated Oxidative Stress Responses. *Antioxidants (Basel)* 2017, *6*, 75.

[71] Ayob, A.Z., Ramasamy, T.S., Cancer stem cells as key drivers of tumour progression. *Journal of Biomedical Science* 2018, *25*, 20.

[72] Dudley, M.E., Wunderlich, J.R., Robbins, P.F., Yang, J.C., et al., Autoimmunity in Patients After Clonal Repopulation with Antitumour Lymphocytes. 2002, *298*, 13.

[73] Disis, M.L., Bernhard, H., Jaffee, E.M., Use of tumour-responsive T cells as cancer treatment. *Lancet* 2009, *373*, 673–683.

[74] Radbruch, A., Thiel, A., Cell therapy for autoimmune diseases: does it have a future? *Ann Rheum Dis* 2004, *63*, ii96–ii101.

[75] Sengupta, N., MacFie, T.S., MacDonald, T.T., Pennington, D., et al., Cancer immunoediting and “spontaneous” tumour regression. 2010, 8.

[76] Osińska, I., Popko, K., Demkow, U., Perforin: an important player in immune response. *Cent Eur J Immunol* 2014, *39*, 109–115.

[77] Bots, M., Medema, J.P., Granzymes at a glance. *J Cell Sci* 2006, *119*, 5011–5014.

[78] Molecular Biology of the Cell (Second Edition) by Bruce Alberts, Dennis Bray, Julian Lewis, et al. (Authors): Very Good Decorative Hardcover (1989) 2nd Edition | gearbooks.

[79] Orange, J.S., Formation and function of the lytic NK-cell immunological synapse. *Nat Rev Immunol* 2008, *8*, 713–725.

[80] Jenkins, M.R., Griffiths, G.M., The synapse and cytolytic machinery of cytotoxic T cells. *Curr Opin Immunol* 2010, *22*, 308–313.

[81] Spontaneous cancer regression of melanoma - Search Results - PubMed [WWW Document],(2022)https://pubmed.ncbi.nlm.nih.gov/?term=spontaneous+cancer+regression+of+melanoma. Accessed 14 June 2022.

[82] Analyze your own microarray data in R/Bioconductor-BITS wiki., 2022. Available from:https://wiki.bits.vib.be/index.php/Analyze_your_own_microarray_data_in_R/Bioconductor.

[83] Ratner, S. (Ed.), Mechanisms of Lymphocyte Extravasation, 1st edition, S. Karger, 1992.

[84] Rousalova, I., Krepela, E., Granzyme B-induced apoptosis in cancer cells and its regulation (review). *Int J Oncol* 2010, *37*, 1361–1378.

[85] Khar, A., Mechanisms involved in natural killer cell mediated target cell death leading to spontaneous tumour regression. *J. Biosci.* 1997, *22*, 23–31.

[86] Martin, R., Teo, K.L., Optimal Control of Drug Administration in Cancer Chemotherapy, WORLD SCIENTIFIC, 1993.

[87] Bayat Mokhtari, R., Homayouni, T.S., Baluch, N., Morgatskaya, E., et al., Combination therapy in combating cancer. *Oncotarget* 2017, *8*, 38022–38043.

[88] Combination Treatments | SEER Training [WWW Document] (2022)https://training.seer.cancer.gov/treatment/combination/?msclkid=b91f81b3ced211ec93f5c37d7391014b. Accessed 8 May 2022.

[89] Tannock, I.F., Combined modality treatment with radiotherapy and chemotherapy. *Radiotherapy and Oncology* 1989, *16*, 83–101.

[90] Hubenak, J.R., Zhang, Q., Branch, C.D., Kronowitz, S.J., Mechanisms of injury to normal tissue after radiotherapy: a review. *Plast Reconstr Surg* 2014, *133*, 49e–56e.

[91] MacDonald, V., Chemotherapy: Managing side effects and safe handling. *Can Vet J* 2009, *50*, 665–668.

[92] Kirkwood, J.M., Butterfield, L.H., Tarhini, A.A., Zarour, H., et al., Immunotherapy of cancer in 2012. *CA: A Cancer Journal for Clinicians* 2012, *62*, 309–335.

[93] Treating Cancer with Immunotherapy | Types of Immunotherapy [WWW Document] (2022) https://www.cancer.org/treatment/treatments-and-side-effects/treatment-types/immunotherapy/what-is-immunotherapy.html. Accessed 8 May 2022

[94] Borghaei, H., Smith, M.R., Campbell, K.S., Immunotherapy of cancer. *European Journal of Pharmacology* 2009, *625*, 41–54.

[95] Cole, W.H., Efforts to explain spontaneous regression of cancer. *J Surg Oncol* 1981, *17*, 201–209.

[96] Salman, T., Spontaneous tumour regression. *Journal of Oncological Science* 2016, *2*, 1–4.

[97] Shannon, P., Markiel, A., Ozier, O., Baliga, N.S., et al., Cytoscape: a software environment for integrated models of biomolecular interaction networks. *Genome Res* 2003, *13*, 2498–2504.

[98] Pathan, M., Keerthikumar, S., Ang, C.-S., Gangoda, L., et al., FunRich: An open access standalone functional enrichment and interaction network analysis tool. *Proteomics* 2015, *15*, 2597–2601.

[99] Szklarczyk, D., Gable, A.L., Lyon, D., Junge, A., et al., STRING v11: protein–protein association networks with increased coverage, supporting functional discovery in genome-wide experimental datasets. *Nucleic Acids Res* 2019, *47*, D607–D613.

[100] Tang, Y., Li, M., Wang, J., Pan, Y., et al., CytoNCA: a cytoscape plugin for centrality analysis and evaluation of protein interaction networks. *Biosystems* 2015, *127*, 67–72.

[101] Kutmon, M., Ehrhart, F., Willighagen, E.L., Evelo, C.T., et al., CyTargetLinker app update: A flexible solution for network extension in Cytoscape. *F1000Res* 2019, *7*, ELIXIR-743.

[102] Wishart, D.S., Feunang, Y.D., Guo, A.C., Lo, E.J., et al., DrugBank 5.0: a major update to the DrugBank database for 2018. *Nucleic Acids Res* 2018, *46*, D1074–D1082.

[103] Wendorff, T.J., Schmidt, B.H., Heslop, P., Austin, C.A., et al., The structure of DNA-bound human topoisomerase II alpha: conformational mechanisms for coordinating inter-subunit interactions with DNA cleavage. *J Mol Biol* 2012, *424*, 109–124.

[104] The Human Protein Atlas [WWW Document] (2022) https://www. proteinatlas.org/. Accessed 6 Feb 2022.

[105] GEPIA (Gene Expression Profiling Interactive Analysis) [WWW Document] (2022) http://gepia.cancer-pku.cn/index.html. Accessed,18 July 22.

[106] Kanehisa, M., Furumichi, M., Tanabe, M., Sato, Y., et al., KEGG: New perspectives on genomes, pathways, diseases and drugs. *Nucleic Acids Research* 2016, *45*.

[107] Dennis, G., Sherman, B.T., Hosack, D.A., Yang, J., et al., DAVID: Database for Annotation, Visualization, and Integrated Discovery. *Genome Biology* 2003, *4*, R60.

[108] Bindea, G., Mlecnik, B., Hackl, H., Charoentong, P., et al., ClueGO: a Cytoscape plug-in to decipher functionally grouped gene ontology and pathway annotation networks. *Bioinformatics* 2009, *25*, 1091–1093.

[109] Jeong, H., Mason, S.P., Barabási, A.-L., Oltvai, Z.N., Lethality and centrality in protein networks. *Nature* 2001, *411*, 41–42.

[110] Freeman, L.C., Borgatti, S.P., White, D.R., Centrality in valued graphs: A measure of betweenness based on network flow. *Social Networks* 1991, *13*, 141–154.

[111] Sabidussi, G., The centrality index of a graph. *Psychometrika* 1966, *31*, 581–603.

[112] Ravindran Menon, D., Luo, Y., Arcaroli, J.J., Liu, S., et al., CDK1 Interacts with Sox2 and Promotes Tumour Initiation in Human Melanoma. *Cancer Res* 2018, *78*, 6561–6574.

[113] Song, L., Robson, T., Doig, T., Brenn, T., et al., DNA repair and replication proteins as prognostic markers in melanoma. *Histopathology* 2013, *62*, 343–350.

[114] Matias-Barrios, V.M., Radaeva, M., Song, Y., Alperstein, Z., et al., Discovery of New Catalytic Topoisomerase II Inhibitors for Anticancer Therapeutics. *Frontiers in Oncology* 2021, *10*.

[115] Zhang, Y., Hunter, T., Roles of Chk1 in Cell Biology and Cancer Therapy. *Int J Cancer* 2014, *134*, 10.1002/ijc.28226.

[116] Shvemberger, I.N., Conversion of Malignant Cells into Normal Ones, in: *International Review of Cytology*, Elsevier, 1986, pp. 341–386.

[117] Kumari, B., Sakode, C., Lakshminarayanan, R., Purohit, P., et al., A mechanistic analysis of spontaneous cancer remission phenomenon: identification of genomic basis and effector biomolecules for therapeutic applicability. *3 Biotech* 2023, *13*, 113.

[118] Pathan, M., Keerthikumar, S., Ang, C.-S., Gangoda, L., et al., FunRich: An open access standalone functional enrichment and interaction network analysis tool. *Proteomics* 2015, *15*, 2597–2601.

[119] Palmieri, G., Ombra, M., Colombino, M., Casula, M., et al., Multiple Molecular Pathways in Melanomagenesis: Characterization of Therapeutic Targets. *Front Oncol* 2015, *5*, 183.

[120] Lo, J.A., Fisher, D.E., The melanoma revolution: from UV carcinogenesis to a new era in therapeutics. *Science* 2014, *346*, 945–949.

[121] Peng, S.-B., Henry, J.R., Kaufman, M.D., Lu, W.-P., et al., Inhibition of RAF Isoforms and Active Dimers by LY3009120 Leads to Anti-tumour Activities in RAS or BRAF Mutant Cancers. *Cancer Cell* 2015, *28*, 384–398.

[122] Kessler, D., Bergner, A., Böttcher, J., Fischer, G., et al., Drugging all RAS isoforms with one pocket. *Future Med Chem* 2020, *12*, 1911–1923.

[123] Alam, S., Khan, F., Virtual screening, Docking, ADMET and System Pharmacology studies on Garcinia caged Xanthone derivatives for Anticancer activity. *Sci Rep* 2018, *8*, 5524.

[124] Kang, D., Pang, X., Lian, W., Xu, L., et al., Discovery of VEGFR2 inhibitors by integrating naïve Bayesian classification, molecular docking and drug screening approaches. *RSC Adv.* 2018, *8*, 5286–5297.

[125] Wu, G., Robertson, D.H., Brooks, C.L., Vieth, M., Detailed analysis of grid-based molecular docking: A case study of CDOCKER-A CHARMm-based MD docking algorithm. *J Comput Chem* 2003, *24*, 1549–1562.

[126] Chen, R., Li, L., Weng, Z., ZDOCK: an initial-stage protein-docking algorithm. *Proteins* 2003, *52*, 80–87.

[127] Balasubramaniyan, S., Irfan, N., Umamaheswari, A., Puratchikody, A., Design and virtual screening of novel fluoroquinolone analogs as effective mutant DNA GyrA inhibitors against urinary tract infection-causing fluoroquinolone resistant Escherichia coli. *RSC Adv.* 2018, *8*, 23629–23647.

[128] Banks, J.L., Beard, H.S., Cao, Y., Cho, A.E., et al., Integrated Modeling Program, Applied Chemical Theory (IMPACT). *J Comput Chem* 2005, *26*, 1752–1780.

[129] Shrivastava, A., Mathur, K., Verma, R.K., Jayadev Magani, S.K., et al., Molecular dynamics study of tropical calcific pancreatitis (TCP) associated calcium-sensing receptor single nucleotide variation. *Frontiers in Molecular Biosciences* 2022, *9*.

[130] MacCorkle, R.A., Tan, T.-H., Mitogen-activated protein kinases in cell-cycle control. *Cell Biochem Biophys* 2005, *43*, 451–461.

[131] Brzezianska, E., Pastuszak-Lewandoska, D., A minireview: the role of MAPK/ERK and PI3K/Akt pathways in thyroid follicular cell-derived neoplasm. *FBL* 2011, *16*, 422–439.

[132] Suski, J.M., Braun, M., Strmiska, V., Sicinski, P., Targeting Cell-cycle Machinery in Cancer. *Cancer Cell* 2021, *39*, 759–778.

[133] Barnaba, N., LaRocque, J.R., Targeting cell cycle regulation via the G2-M checkpoint for synthetic lethality in melanoma. *Cell Cycle*., *20*, 1041–1051.

[134] Omholt, K., Platz, A., Kanter, L., Ringborg, U., et al., NRAS and BRAF mutations arise early during melanoma pathogenesis and are preserved throughout tumour progression. *Clin Cancer Res* 2003, *9*, 6483–6488.

[135] Robertson, G.P., Functional and therapeutic significance of Akt deregulation in malignant melanoma. *Cancer Metastasis Rev* 2005, *24*, 273–285.

[136] Li, H.-L., Ma, Y., Zheng, C.-J., Jin, W.-Y., et al., Exploring the effect of D61G mutation on SHP2 cause gain of function activity by a molecular dynamics study. *J Biomol Struct Dyn* 2018, *36*, 3856–3868.

[137] Świstowska, M., Gil-Kulik, P., Krzyżanowski, A., Bielecki, T., et al., Potential Effect of SOX2 on the Cell Cycle of Wharton's Jelly Stem Cells (WJSCs). *Oxid Med Cell Longev* 2019, *2019*, 5084689.

[138] Pu, L., Su, L., Kang, X., The efficacy of cisplatin on nasopharyngeal carcinoma cells may be increased via the downregulation of fibroblast growth factor receptor 2. *Int J Mol Med* 2019, *44*, 57–66.

[139] Dimco, G., Knight, R.A., Latchman, D.S., Stephanou, A., STAT1 interacts directly with cyclin D1/Cdk4 and mediates cell cycle arrest. *Cell Cycle* 2010, *9*, 4638–4649.

[140] Qian, J., Liu, H., Wei, S., Liu, Z., et al., Association between putative functional variants in the PSMB9 gene and risk of melanoma - re-analysis of published melanoma genome-wide association studies. *Pigment Cell Melanoma Res* 2013, *26*, 10.1111/pcmr.12069.

[141] Kołat, D., Kałuzińska, Ż., Bednarek, A.K., Płuciennik, E., The biological characteristics of transcription factors AP-2α and AP-2γ and their importance in various types of cancers. *Biosci Rep* 2019, *39*, BSR20181928.

[142] Banerji, U., Affolter, A., Judson, I., Marais, R., et al., BRAF and NRAS mutations in melanoma: potential relationships to clinical response to HSP90 inhibitors. *Molecular Cancer Therapeutics* 2008, *7*, 737–739.

[143] Heppt, M.V., Siepmann, T., Engel, J., Schubert-Fritschle, G., et al., Prognostic significance of BRAF and NRAS mutations in melanoma: a German study from routine care. *BMC Cancer* 2017, *17*, 536.

[144] Thomas, N.E., Edmiston, S.N., Alexander, A., Groben, P.A., et al., Association Between NRAS and BRAF Mutational Status and Melanoma-Specific Survival Among Patients With Higher-Risk Primary Melanoma. *JAMA Oncology* 2015, *1*, 359–368.

APPENDIX-I

Formulation of System design using control system analysis:

State variables, control variables, and constraint conditions are the three fundamental pillars of a control system, which is required to design any system.

- *State variables* of our system are the internal biological parameters. Here we are going to formulate our ordinary differential equations in terms of a control system using a multimodel compartmental model. Here in figure 2.4 of text (chapter 2), the state variables are (1) Interleukin-2 concentration in blood (C), (2) DNA damage factor (D), (3) Tumour infiltrating lymphocytes (A), (4) Natural killer cells (K), (5) Circulating lymphocytes (B), and (6) the malignant tumour cells (M). These states variables are represented as a function of $X_{n,}$ where n = 1 to 6.

- *Control variables* of our system are the external administration of 3 the anti-tumour agents i.e. (1) DNA damage factor generation rate (v_D *(t)*), (2) interleukin-2 formation rate (v_C *(t)*) and (3) tumour infiltrating lymphocytes formation rate (v_A *(t)*). These control variables are represented as a function of $U_{m,}$ where m = 1 to 3.

- The quantitative specifications of physiological thresholds that the cancer regression process cannot cross are known as the *constraint conditions* of the system. The minimum and maximum values for each state variable must be preserved within normal physiological bound (Table 2.2 of chapter 2).

Step 1: Tumour cell module:

Let us consider Figure 2.4 of chapter 2, the objective here is to find out the desired value of $D^{\ddagger}$ and $A^{\ddagger}$ which are the input parameters for tumour cell module, which will enable the tumour (M) cell output module to have the desired value M^{*} in time point t_p [Figure 2.1 (b)]. The rate equation for the output state variable, tumour cell population M, regarding the tumour cell module in Figure 2.4. is obtained by expressing its time derivative M': firstly, in terms of the state function $f_M(X_n)$, where X_n is the state variables due to two intrinsic biological parameters (i) logistic tumour cell growth parameter, and (ii) tumour cell elimination parameter due to natural killer cells. And secondly, in terms of module's input, we define the therapy variables g_{M1} and g_{M2} that represents the dose-response saturation behavior (Ur) of two antitumour entities: DNA blockage factor D and cytotoxic T-cell population A.

Thus, $$M' = f_M + [g_{M1}U_D + g_{M2}U_A] \quad (1)$$

$$\Rightarrow M' = f_M + b_M \quad \ldots\ldots(\text{where } b_M = [g_{M1}U_D + g_{M2}U_A]) \quad (2)$$

Here, U_D and U_A represents the efficacy of the anti-tumour therapeutic entities of DNA blockage factor and cytotoxic T-cell respectively, while b_M is the combined effect of these two anti-tumour entities on tumour growth rate M'. This quantitatively antitumour behaviour of eq. (1) is a saturation type of dose-response function, which is a common characteristic of pharmacological chemical reactions (such Michaelis-Menten function, Hill function, or similar activity function). As a result, Eq. (1), which corresponds to Eq. (7) of main text, can be expressed using Michaleis-Menten Kinetics as,

$$M' = aM(1 - bM) - cKM - QM - k_M(1 - e^{-D})M \quad (3)$$

Comparing the right side of eq. (1) and (3), we see that

$$\left.\begin{aligned} f_M &= [aM(1 - bM) - cKM] \\ g_{M1} &= -k_M M \\ g_{M2} &= -M \end{aligned}\right\} \quad (4)$$

and

$U_D = (1 - e^{-D})$; and $U_A = Q = [(d\,A^l) / (sM^l + A^l)]$ (5)

Now, we employ the previously defined tumour growth rate [namely $M' = -\kappa_M(M - M^*)$] in chapter 1 to enforce the tumour eradication using the trajectory tracking approach mentioned earlier in chapter 1. Using this statement of $M' = -\kappa_M(M - M^*)$ in equation (1), we can determine the prerequisite for inducing total tumour regression as:

$$f_M + g_{M1}U_D + g_{M2}U_A = -\kappa_M(M - M^*) \quad (6)$$

$$\Rightarrow g_{M1}U_D + g_{M2}U_A = -\kappa_M(M - M^*) - f_M$$

$$\Rightarrow g_{M1}U_D + g_{M2}U_A = b_M \quad (7)$$

where, $b_M = -\kappa_M(M - M^*) - f_M = -[\kappa_M(M - M^*) + f_M]$ (8)

$$\Rightarrow f_M + \kappa_M(M - M^*) + b_M = 0 \quad (9)$$

According to Eq. (8), for effective therapy, the combined therapy-induced anti-tumour effect term, b_M, should address two factors: first, the condition necessary for enforcing the elimination of the tumour cell population, represented by the expression - $\kappa_M(M - M^*)$, and second, the growth of the tumour cell population as a result of biological processes, represented by f_M. According to Eq. (8), the relaxation decay term, b_M, has a negative value if the tumour is going to regress (or a zero value if the tumour is arrested at a specific volume and remains stable), therefore in this case, $b_M \leq 0$. From Eq. (7)

$$g_{M1}U_D + g_{M2}U_A - b_M = 0 \quad (10$$

Eq. (7) shows the link between the blood levels concentration of the antitumour agents (U_D and U_A), which, if these levels are attained, will ensure that the tumour cells are completely disappear. However, it is also necessary to maintain the blood levels of U_D and U_A so that their combined toxicity on the patient is kept to a minimum.

Therefore, we must now reduce the normal tissue damage in term of a damage cost function due to anti-tumour entities. So, we need to minimize the toxicity of these antitumour agents.

Toxicity minimization of antitumour entities:

The cost function for the tumour cell compartment can be calculated using the quadratic cost parameter J_M (chapter 1) as follows:

$$J_M = \tfrac{1}{2} (r_{M1} U_D^2 + r_{M2} U_A^2) \qquad (11)$$

Here the weighting factors used in this instance for the two antitumour entities, DNA blockage factor and cytotoxic T-cells, are r_{M1} and r_{M2}. In addition to minimizing the cost function J_M, eq. (7) should also be followed as a constraint. Evidently a constrained optimization problem, the minimization of the cost function, $J_M = \tfrac{1}{2} (r_{M1} U_D^2 + r_{M2} U_A^2)$, may be addressed optimally using the Lagrange multiplier (λ),

Thus, the augmented cost function $\underline{J}$ can be expressed as follows:

$$\underline{J} = \tfrac{1}{2} [r_{M1} U_D^2 + r_{M2} U_A^2] + [\lambda \{ g_{M1} U_D + g_{M2} U_A - b_M \}] \qquad (12)$$

Thence, apropos the Lagrange's technique, the right-sided expression in eq. (12) enclosed by the second brackets {…} includes the left side of the constraint equation [eq. (10)]. We differentiate $\underline{J}$ with respect to the two variables U_D and U_A for the minimization of the augmented cost function. The minimization criteria are thus found out to be $\partial \underline{J} / \partial U_D = 0$ and $\partial \underline{J} / \partial U_A = 0$, from which we derive the equations for the two variables U_D and U_A as follows:

a) ***Efficacy of DNA blockage factor, U_D:***

As, $U_A = (b_M - g_{M1} U_D) / g_{M2}$ …..(using eq. (10))

So, by putting above U_A value in eq. 12, it will become

$$\underline{J} = \tfrac{1}{2} [r_{M1} U_D^2 + r_{M2} \{(b_M - g_{M1} U_D) / g_{M2}\}^2] + [\lambda \{ g_{M1} U_D + g_{M2} ((b_M - g_{M1} U_D)/ g_{M2}) - b_M \}]$$

……(12A)

Now, by using $\partial \underline{J} / \partial U_D = 0$, eq. 12 (A) becomes

$\Rightarrow \quad ½ [\, 2r_{M1} U_D + 2r_{M2} ((b_M - g_{M1} U_D) / g_{M2}) (-g_{M1} / g_{M2})] = 0$

$\Rightarrow \quad r_{M1} U_D - [\{r_{M2} g_{M1} ((b_M - g_{M1} U_D)\}/(g_{M2})^2] = 0$

$\Rightarrow \quad r_{M1} U_D - [\{r_{M2} g_{M1} b_M - r_{M2} (g_{M1})^2 U_D)\}/(g_{M2})^2] = 0$

$\Rightarrow \quad U_D [r_{M1} + \{r_{M2}(g_{M1})^2\} / (g_{M2})^2] = [(r_{M2} g_{M1} b_M)/(g_{M2})^2]$

$\Rightarrow \quad U_D [r_{M1} (g_{M2})^2 + \{r_{M2}(g_{M1})^2\}] = (r_{M2} g_{M1} b_M)$

$\Rightarrow \quad U_D = (r_{M2} g_{M1} b_M) / [r_{M1} (g_{M2})^2 + \{r_{M2}(g_{M1})^2\}]$

$\Rightarrow \quad U_D = (g_{M1} b_M) / r_{M1} [(g_{M2})^2 / r_{M2} + (g_{M1})^2 / r_{M1}]$

$\Rightarrow \quad U_D = b_M g_{M1} / r_{M1} \mathrm{G}$ ... This is the efficacy of DNA blockage factor (13)

a) Eefficacy of cytotoxic T-cell U_A:

$\Rightarrow \quad U_A = b_M g_{M2} / r_{M2} \mathrm{G}$ (14)

where, $\mathrm{G} = [(g_{M1})^2 / r_{M1} + (g_{M2})^2 / r_{M2}]$ (15)

Also from eq. (5)

$U_D = (1 - e^{-D})$; and $U_A = (d A^l) / (s M^l + A^l)$ (16)

By solving the above two equations of eq. (16), we will get the desired antitumour entity input level for tumour cell input module.

i.e. $D^{\ddagger} = -ln(1 - U_D)$; $A^{\ddagger} = [s M^l U_A / (d - U_A)]^{1/l}$ (17)

where $D^{\ddagger}$ and $A^{\ddagger}$ are desired value of two antitumour entities (i.e. blood concentration of DNA blockage factor and of cytotoxic T-cell). Further, by substituting the value of U_D and U_A from eq. (13) and (14) into eq. 17; we can arrived at the desired value of DNA blockage factor and cytotoxic T-cell population.

i.e. $D^{\ddagger} = -ln[1 - \{b_M g_{M1} / r_{M1} \mathrm{G}\}]$ (18)

and, $A^{\ddagger} = [s M^l (b_M g_{M2} / r_{M2} \mathrm{G}) / \{d - (b_M g_{M2} / r_{M2} \mathrm{G})\}]^{1/l}$ (19)

Step 2: Cytotoxic T-cell module:

The goal here is to find the desired values for this module's input parameters namely, the interleukin-2 blood level and tumour-infiltrating lymphocyte formation rate, $C^{\ddagger}$ and $v_A^{\ddagger}$, will induce the output (the cytotoxic T-cell population, A) to be driven to the desired value $A^{\ddagger}$. When all of the tumour cells have been destroyed at time point t_F (Figure 2.1 (b), chapter 2), this enforced driving must be more rapid than the previous module (tumour cell module).

Here also, we employ the trajectory guided tracking principle of control systems analysis, which we have already applied to the tumour cell module. Similarly, by applying the same reasoning behind the lowering of the deviation or error [as describe in chapter 1, section 1.4], we obtain:

$$A' = -\kappa_A(A - A^{\ddagger}) \tag{20}$$

Now we consider the tumour cell module's characteristic rate, $M' = f_M(X_n) + b_M$ [i.e., eq. (1) of this Appendix-I]. We now desire to express this rate formulation in terms of A', the rate of change of the cytotoxic T-cell module. So, using Eq. 6 of chapter 2, we express the temporal dynamics equation of A' as:

$$A' = f_A(X) + U_C + v_A \tag{21}$$

where $f_A(X)$ is a system function representing the T-cell immunomodulation, i.e., the biological factors acting on this cytotoxic T-cell population, and v_A is the tumour-infiltrating lymphocyte formation rate. U_C is the therapeutic efficacy of interleukin-2. By comparing eq. 21 above and eq. 6 (chapter 2), we arrived at:

$$A' = dA/dt = -mA + Aj[(Q^2M^2) / (k + Q^2M^2)] - qAM + (r_1K + r_2B)M - uKA^2 - k_A(1 - e^{-D})A$$

$$+ \{p_c AC / (g_C + C) + v_A(t)\} \tag{22}$$

With reference to this comparison, it is noted that the term U_C, which refers to interleukin efficacy level C, can be defined as:

$$U_C = (p_c AC) / (g_C + C) \tag{23}$$

Whereby we obtain,

$$f_A(X) = -mA + Aj[(Q^2M^2) / (k + Q^2M^2)] - qAM + (r_1K + r_2B)M - uKA^2 - k_A(1 - e^{-D})A \tag{24}$$

Also, from eq. (20) and (21), we have

$$f_A(X) + U_C + v_A = -\kappa_M(A - A^{\ddagger})$$

$$\Rightarrow \quad U_C + v_A = -f_A(X) - \kappa_M(A - A^{\ddagger})$$

$$\Rightarrow \quad U_C + v_A = b_A \tag{25}$$

Here, $b_A = -f_A(X) - \kappa_M(A - A^{\ddagger})$ (26)

Note that the last two terms of eq. 22 (within {…}), are terms about input of the antitumour entities, respectively dependent on interleukin and tumour-infiltrating lymphocyte [denoted as b_A in eq. (26)]. The second term of the {…} expression is the tumour infiltrating leucocytes formation rate (denoted as v_A), and the first term (($p_c AC$) / ($g_C + C$)) is the therapeutic efficacy of interleukin-2. And the remaining part of eq. 22 is $f_A(X)$, which is the performance function of the cytotoxic T-cell module.

Indeed, the aforementioned eq. (22) shows that if the tumour regresses (or if the tumour is halted and hence stable), $b_M \geq 0$, the relaxation decay term b_A has a positive value. In fact, equation (25), if used, will ensure the complete eradication of the tumour, and this equation relates with the features of the antitumour agents interleukin and tumour infiltrating lymphocytes (U_C and v_A). For this module, the two antitumour agents are interleulin-2 (its efficacy function is U_C) and tumour infiltrating leucocytes (its formation

rate, v_A), Thus, like the earlier tumour module we again need to minimize the toxicity of these antitumour agents.

Toxicity minimization of antitumour agents:

The cost function for the cytotoxic T-cell module is as follows:

$$J_A = \tfrac{1}{2} (r_{A1} U_C^2 + r_{A2} v_A^2) \quad (27)$$

where the two antitumour entities present in this module are responsible for the sensitivity weights r_{A1} and r_{A2}. The constraint requirement [$U_C + v_A = b_C$] from [eq. (25)] need to be followed for minimization. With the use of the Lagrange multiplier method, we can solve for:

the augmented cost function $\underline{J}$ which can be expressed as follows:

$$\underline{J} = \tfrac{1}{2} (r_{A1} U_C^2 + r_{A2} v_A^2) + [\lambda \{ U_C + v_A - b_A \}] \quad (28)$$

The minimization criteria are thus found to be $\partial \underline{J} / \partial U_C = 0$ and $\partial \underline{J} / \partial v_A = 0$, from which we derive the equations for the two variables U_C and v_A as follows:

a) Antitumour efficacy of Interleukin-2 U_C:

We note, $v_A = (b_A - U_C)$ .....(using eq. (25))

Thence, by putting the above v_A value in eq. 28, we have

$$\underline{J} = \tfrac{1}{2} (r_{A1} U_C^2 + r_{A2} (b_A - U_C)^2) + [\lambda \{ U_C + (b_A - U_C) - b_A \}]$$

Now, by using $\partial \underline{J} / \partial U_C = 0$, we arrive at;

$$\tfrac{1}{2} [2 r_{A1} U_C + 2 r_{A2} \{ (b_A - U_C) (-1) \}] = 0$$

$$\Rightarrow \quad r_{A1} U_C + r_{A2} (U_C - b_A) = 0$$

$$\Rightarrow \quad U_C (r_{A1} + r_{A2}) = r_{A2} b_A$$

$\Rightarrow \quad U_C = r_{A2}\, b_A / (r_{A1} + r_{A2})$

$\Rightarrow \quad U_C = r_{A2}\, b_A / r_{A1}\, r_{A2}\, (1/r_{A2} + 1/ r_{A1})$

$\Rightarrow U_C = b_A / r_{A1}\, (1/ r_{A1} + 1/ r_{A2})$

$\Rightarrow \quad U_C = b_A / r_{A1}\mathrm{H}$ ... This expression is the clinical efficacy of IL-2 (29)

b) Efficacy of tumour infiltrating lymphocyte is, v_A:

Likewise, we obtain the efficacy of these lymphocytes:

$$v_A = b_A / r_{A2}\mathrm{H} \tag{30}$$

where, $\mathrm{H} = [1/ r_{A1} + 1/ r_{A2}]$ (31)

Also from eq. (23), we have

$$C^{\ddagger} = g_C\, U_C / (p_C A - U_C) \tag{32}$$

Note that here $C^{\ddagger}$ is the desired value of antitumour entity (i.e. blood concentration of IL-2). Moreover, by substituting the value of U_C from eq. (29) into eq. (32), we obtain at the desired value of the formation rate of tumour-infiltrating leucocyte:

i.e. $C^{\ddagger} = g_C\, b_A / (p_C A\, r_{A1}\mathrm{H} - b_A)$ (33)

Step 3: DNA damage module:

In this case, the objective is to determine the desired value, $v_D^{\ddagger}$, of the module's input parameter (DNA damage factor), which would drive the module's output i.e. blood concentration of the DNA damage factor D to reach the desired value, $D^{\ddagger}$, [eq. (18)] within the time point t_F (Figure 2.1 (b)), this driving must be completed faster than the prior module (the T-cell module).

The requirement that $E_D' + k_D\, E_D = 0$ (from chapter 1, section 1.4), must be put into practice, with the deviation $E_D = (D - D^{\ddagger})$. Furthermore, we obtain $D' = -k_D\, (D - D^{\ddagger})$ using

the same logic as the earlier module. After removing D′ from both this equation and equation (2) of chapter 2, we arrive at:

$$v_D^{\ddagger} = \gamma D - k_D (D - D^{\ddagger}) \quad (34)$$

(where $v_D^{\ddagger}$ is the desired level of DNA damage factor generation rate)

Step 4: Interleukin-2 injection module:

The requirement to be implemented here is that $E_C' + k_C E_C = 0$, where $E_C = (C - C^{\ddagger})$, here E_C denotes the deviation. Hence $C' = -k_C (C - C^{\ddagger})$. Using eq. (1) of chapter 1 to eliminate C', we obtain the desired Interleukin 2 formation rate;

$$v_C^{\ddagger} = \mu_C C - k_C (C - C^{\ddagger}) \quad (35)$$

Step 5: Tumour infiltrating leucocyte module:

For this module, eq. (30) can be written as,

$$v_A^{\ddagger} = b_A / r_{A2}\mathrm{H} \quad (36)$$

This $v_A^{\ddagger}$ term is the required Tumour infiltrating leucocyte generation rate.

To sum up, if the formation rate of the three antitumour entities (DNA impairment factor, T- lymphocyte cell, and Interleukin-2) attains the respectively desired values with time ($v_D^{\ddagger}$, $v_A^{\ddagger}$, and $v_C^{\ddagger}$), then the malignant cell population will undergo permanent complete regression and extinct.

APPENDIX-II

Formulating of the Profile of Antitumour Entities

PART-A

Analysis of appropriate antitumour weights (r_{M1}, r_{M2}, and r_{A1}, r_{A2})

The tuning parameters r_{M1}, r_{M2}, r_{A1}, and r_{A2}, are the adjustable intensity weights of the antitumour agents, selection of proper values of the weights are necessary to reduce the toxicity cost. These functional weights are acting at the two stages.

(i) At tumour cell module: the weights r_{M1}, and r_{M2} respectively are the antitumour efficiency weight of (a) DNA blockage factor and of (b) Cytotoxic T-cell;

(ii) At Cytotoxic T-cell module: here the weights r_{A1}, and r_{A2} respectively are the antitumour efficiency weight of (a)T-cell activation weight (activated by Interleukin-2) and (b) tumour infiltrating leucocytes.

The tuning parameter values must be larger than or equal to zero since they relate to actual cellular and biochemical processes and flow rates. They cannot have imaginary or fixed values. They are continuously changed as the tumour regression process advances to reduce toxicity for the patient, while simultaneously forcing the tumour cell population to zero. It turns out that the ratio r_{M1}: r_{M2} is the basic factor to consider in these optimization situations. The aim is to appropriately select or optimize the value of the other tuning parameter, r_{M2}, by taking that the parameter r_{M1} has a normalized value of unity (i.e., $r_{M1} = 1$). Furthermore, the other ratio r_{A1}: r_{A2} follows the same reasoning. As a result, we can use the following values for two of the parameters: $r_{M1} = 1$ and $r_{A1} = 1$.

Calculation of other two tuning parameters (r_{M2} and r_{A2}):

The values of the tuning parameters r_{M2} and r_{A2} can be selected based on certain physical conditions of the antitumour entities (U_D, U_A, and U_C) and their corresponding control variables (v_D, v_A and v_C).

Step 1: Boundary conditions of DNA blockage efficacy factor U_D

We now examine the DNA blockage factor, which affects the tumour cell population module (Figure 2.4, chapter 2) and where the tuning parameters or weights (r_{M1} and r_{M2}) are related to the toxicity cost J_M [see Appendix-I. Eq. (11)]. The tuning parameter range for the DNA blockage factor will be now analyzed; this range of values will allow for adjusting the tuning weight to ensure total tumour eradication.

***Upper bound of U_D*:**

From eq. 17 of Appendix-1,

$$D^{\ddagger} = -ln(1- U_D) \tag{1}$$

Where $D^{\ddagger}$ is the desired value of the blood concentration of DNA blockage factor. The clinical efficacy parameter $D^{\ddagger}$ needs to avoid having imaginary values. Also, since logarithm is not defined for zero or negative values, therefore, the upper bound of U_D is 1.

***Lower bound of U_D*:**

From eq. (34) of Appendix-I, $v_D^{\ddagger}(t) = \gamma D - k_D (D - D^{\ddagger})$. Since $v_D^{\ddagger}(t)$ is the DNA blockage factor generation rate, it cannot be negative and hence $v_D^{\ddagger}(t) \geq 0$.

Therefore, $\gamma D - k_D (D - D^{\ddagger}) \geq 0$ (2)

By putting $D^{\ddagger}$ value from eq. (1) to eq. (2), we obtain:

$$\gamma D - k_D (D + ln(1 - U_D)) \geq 0$$

$$\Rightarrow U_D \geq 1 - \exp [(\gamma D / k_D) - D] \quad (3)$$

Thus, this value can be taken as the lower bound of U_D.

Step 2: Boundary conditions of the antitumour weight factor r_{M2}:

Lower bound of r_{M2}:

From eq. (13) of Appendix-I, we have already found the relationship between U_D and tuning parameters r_{M1} and r_{M2} as follows:

$$U_D = b_M g_{M1} / r_{M1} G \quad (4)$$

where, $G = [(g_{M1})^2 / r_{M1} + (g_{M2})^2 / r_{M2}]$ From eq. (3) and eq. (4), we have

$$b_M g_{M1} / r_{M1} G \geq 1 - \exp [(\gamma D / k_D) - D] \quad (5)$$

Also, from eq. 8 of Appendix-I, b_M has a negative value. By transposing eq. (5), we have the lower bound of r_{M2}:

$$r_{M2} \geq (g_{M1})^2 r_{M1} / [\{b_M g_{M1} / 1 - \exp (\gamma D / k_D) - D)]\} - (g_{M1})^2] \quad (6)$$

Upper bound of r_{M2}:

As discussed in upper two section $U_D < 1$. Further, we obtain $b_M \leq 0$, from eq. (5) of the above paragraph. Thereby we get

$$b_M g_{M1} / r_{M1} G < 1 \quad [\text{where } G = [(g_{M1})^2 / r_{M1} + (g_{M2})^2 / r_{M2}]] \quad (7)$$

By transposing eq. (7), we arrive at:

$$r_{M2} < (g_{M2})^2 r_{M1} / [b_M g_{M1} - (g_{M1})^2] \quad (8)$$

From eq. (6) and eq. (8), we obtain the range of r_{M2} as,

$$(g_{M1})^2 r_{M1} / [\{b_M g_{M1} / 1 - \exp(\gamma D / k_D) - D)]\} - (g_{M1})^2] \leq r_{M2} < (g_{M2})^2 r_{M1} / [b_M g_{M1} - (g_{M1})^2]$$

……(9)

Now, let us consider A and B to be the left and right sides of the inequality of eq. (9), i.e.

$$A = (g_{M1})^2 r_{M1} / [\{b_M g_{M1} / 1 - \exp(\gamma D / k_D) - D)]\} - (g_{M1})^2] \quad (9\ A)$$

$$B = (g_{M2})^2 r_{M1} / [b_M g_{M1} - (g_{M1})^2] \quad (9\ B)$$

As we know that for tumour to regress b_M should be negative and if b_M is positive the tumour should progress. Therefore, for tumour cell to regress: $b_M \leq 0$, then the range of r_{M2} become,

$$A \leq r_{M2} < B \quad (10)$$

In contrast, if tumour is progressing $b_M > 0$, then the range of r_{M2} become

$$A \geq r_{M2} > B \quad (11)$$

Step 3: Boundary conditions for using tumour infiltrating lymphocyte formation rate (v_A)

Here, we focus on tumour-infiltrating leucocyte, which activates cytotoxic T-cells to act through the tumour cell population module (Figure 2.4 of chapter 2). In this module the toxicity cost J_M is correlated with the tuning parameters or weights, r_{M1} and r_{M2} [refer to the section after eq. (11) in the Appendix-I]. We now determine the tuning parameter range that will allow the DNA blockage factor to function efficaciously. This range of values of the tuning parameter will allow us to adjust the tuning weight in order to completely eradicate the tumour.

Step 4: Boundary conditions of the cytotoxic T-cell efficacy factor U_A

Upper bound of U_A

From eq. (17) of Appendix-I, the desired value of cytotoxic T-cell population is,

$$A^{\ddagger} = [s\, M^{l}\, U_A / (d - U_A)]^{1/l} \tag{12}$$

Since $A^{\ddagger}$ is effective at enhancing the elimination of tumours, its clinical efficacy U_A cannot be negative i.e. $U_A \geq 0$ (see the numerator of eq. (12)). The denominator also cannot be zero or negative since $A^{\ddagger}$ is a positive finite cellular population, which implies that $U_A \neq d$ and $d - U_A > 0$ (i.e., $U_A < d$). It should be noted that the parameter d, which represents the upper limit of the U_A, is positive because it represents the saturation level of fractional tumour cell destruction by cytotoxic T-cells.

Lower bound of U_A

From the aforesaid paragraph, we can adopt the range of U_A as follows:

$$0 \leq U_A < d \tag{13}$$

Now, for the range of r_{M2}, we can take eq. (14) of Appendix-1, $U_A = b_M\, g_{M2} / r_{M2}\mathrm{G}$, where $\mathrm{G} = [\, (g_{M1})^2 / r_{M1} + (g_{M2})^2 / r_{M2}]$. Putting this value of U_A in eq. (13)', we have

$$0 \leq b_M\, g_{M2} / r_{M2}\mathrm{G} < d$$

Whereby, $b_M\, g_{M2} / r_{M2}\mathrm{G} > 0$, and $b_M\, g_{M2} / r_{M2}\mathrm{G} < d$. Now, by taking the reciprocal of these two inequalities, we arrive at:

$$r_{M2} \leq \infty \quad \text{and} \quad b_M\, g_{M2} / d\mathrm{G} < r_{M2}$$

i.e., $$b_M\, g_{M2} / d\mathrm{G} < r_{M2} \leq \infty \tag{14}$$

Step 5: Boundary conditions of antitumour effect term b_M:

From eq. 14, we can take $C = b_M g_{M2} / dG$ and $D = \infty$ (14 A)

So, from eq. (14) and eq. (14-A), we can delineate that

Case-1. For tumour regression, $b_M \leq 0$, also $C < r_{M2} \leq D$ (15)

Case-2. For tumour progression, $b_M \geq 0$, also $C > r_{M2} \geq D$ (16)

Step 6: Boundary conditions of T-cell activation effect term $\{b_A\}$:

The interleukin efficacy U_C and the tumour-infiltrating lymphocyte administration term v_A are two immunological inputs that together provide the entire effect of cytotoxic T-cell activation represented by the symbol b_M. We may recall that the desired cytotoxic T-cell value $A^{\ddagger}$ determines the generation rates of T-lymphocytes and Interleukin-2, $v_A(t)$ and $v_C(t)$ (Figure 2.4 of chapter 2). Hence, one may consider that eqs. (15) and (16) are prerequisites for providing the input rate of tumour-infiltration leukocyte and interleukin-2, respectively.

Also, we have $v_A(t) \geq 0$ (17)

because the dose-rate $v_A(t)$ cannot be negative. Further, eq. (30) of Appendix-I states that,

$$v_A = b_A / r_{A2} H \tag{18}$$

where, $H = [1/ r_{A1} + 1/ r_{A2}]$. As the therapeutic weight factor (r_{A1} and r_{A2}) have positive value, so H should be a positive quantity. Now, by substituting eq. (18) in eq. (17), we get

$$b_A / r_{A2} H \geq 0 \tag{19}$$

Given that both r_{A2} and H are positive, eq. (19) indicates that:

$$b_A \geq 0 \qquad (20)$$

Moreover, from eqs. 24 and 26 from Appendix-I, we have

$$b_A = -f_A(X) - \kappa_M(A - A^{\ddagger}) \qquad (21)$$

where,

$$f_A(X) = -mA + Aj[(Q^2M^2) / (k + Q^2M^2)] - qAM + (r_1K + r_2B)M - uKA^2 - k_A(1 - e^{-D})A$$

……(22)

Now, by substituting the value of b_A from eq. 20 into eq. 21, we can get the condition of control process, namely

$$-[-mA+Aj[(Q^2M^2)/(k+Q^2M^2)]-qAM+(r_1K+r_2B)M-uKA^2-k_A(1-e^{-D})A+\kappa_M(A - A^{\ddagger}) \geq 0$$

…….(23)

In the last term of eq. 23, the value of $A^{\ddagger}$ (i.e. the desired value of cytotoxic T-cell population) is given by the eq. 17 of Appendix-I, i.e.

$$A^{\ddagger} = [s\, M^l\, U_A / (d - U_A)]^{1/l} \qquad (24)$$

Putting this value of $A^{\ddagger}$ in eq. 23, we get

$$U_A \geq (d\, P^l) / (s\, M^l + P^l) \qquad (25)$$

Where, U_A is the cytotoxic T-cell efficacy factor and

$P = \mathrm{A} + (1/ k_A) [-mA+Aj[(Q^2M^2)/(k+Q^2M^2)]-qAM+(r_1K+r_2B)M-uKA^2-k_A(1-e^{-D})A]$

Earlier, we have seen that

$U_A = b_M\, g_{M2} / r_{M2}\mathrm{G}$ (from eq. 14 of Appendix-I)

By putting the value of P and U_A in eq. 25, from last two equations, we get the condition of the weighting factor of cytotoxic T-cell, r_{M_2}, in terms of the weighting factor of DNA blockage factor (r_{M_1}), namely

$$r_{M_2} \leq [\{[(s\, M^l + P^l)/ (d\, P^l)]\, b_M\, G_{M2} - (G_{M2})^2\}\, r_{M_1}]/ (G_{M1})^2 \qquad (26)$$

where $G_{M1} = -k_M M$, $G_{M2} = -M$ (as per eq. (4) of Appendix-I)

Now, we can also write eq. (26) as $r_{M_2} \leq E$ (27)

where $E = [\{[(s M^I + P^I)/(d P^I)]\ b_M G_{M2} - (G_{M2})^2\}\ r_{M_1}]/(G_{M1})^2$ (28)

Also, from the second paragraph of this Appendix-I , $r_{M_1} = 1$ in eq. 28. Thus eq. 27 is the sufficient condition for the weight r_{M_2} regarding the tumour infiltrating lymphocyte formation rate, $v_A(t) \geq 0$.

Step 7: Boundary conditions for using Interleukin-2 formation rate (v_C)

As from eq. 32 of Appendix-I, the desired concentration of Interleukin-2, $C^{\ddagger}$, for the complete elimination of tumour is:

$$C^{\ddagger} = g_C U_C / (p_C A - U_C) \quad (29)$$

Here the denominator should not be zero, as $C^{\ddagger}$ should have a real value, i.e.

$$U_C \neq p_C A \quad (30)$$

Also the clinical efficacy of interleukin is defined by eq. (29) of Appendix-I as,

$$U_C = b_A / r_{A1} \mathrm{H} \quad (31)$$

where H = $[1/ r_{A1} + 1/ r_{A2}]$. By substituting eq. (31) in eq. (30), rearranging, we obtain the required value of r_{A2} (the weighting factor of tumour infiltrating lymphocyte), i.e.

$$r_{A2} \neq p_C A r_{A1} / b_A - p_C A \quad (32)$$

where $\mathrm{F} = p_C A r_{A1} / b_A - p_C A$ (33)

So, $r_{A2} \neq \mathrm{F}$ (33 A)

For the interleukin-2 generation rate, $v_C(t)$, eq. (33 (a)) is the necessary condition. Further, $v_C(t)$ should not be negative, whereby we have another requirement:

$$v_C(t) \geq 0 \quad (34)$$

Now we consider the desired interleukin-2 formation rate for tumour elimination $v_C^{\ddagger}$ [eq. (35 of Appendix-I)]:

$$v_C^{\ddagger} = \mu_C\, C - k_C\,(C - C^{\ddagger}) \tag{35}$$

Since $v_C^{\ddagger} \geq 0$, since $v_C^{\ddagger}$ is the desired IL-2 production rate; so eq. (35 of Appendix-I) becomes

$$\mu_C\, C - k_C\,(C - C^{\ddagger}) \geq 0 \tag{36}$$

Also the desired interleukin blood level from eq. 32 of Appendix-I is

$$C^{\ddagger} = g_C\, U_C / (p_C A - U_C) \tag{37}$$

where U_C is given by the eq. (29) of Appendix-I:

$$U_C = b_A / r_{A1}\mathrm{H} \tag{38}$$

Here H = $(1/ r_{A1} + 1/ r_{A2})$ [see eq. (31) of Appendix-I]. Moreover, from eq. (38) above, b_A is the cytotoxic T-cell activation term and can be obtained from eq. (26) of Appendix-I as,

$$b_A = -f_A(X) - \kappa_M(A - A^{\ddagger}) \tag{39}$$

In eq. (39), we have the term $f_A(X)$, which is from eq. 24 of Appendix-I, is:

$$f_A(X) = -mA + Aj[(Q^2M^2)/(k + Q^2M^2)] - qAM + (r_1K + r_2B)M - uKA^2 - k_A(1 - e^{-D})A \tag{40}$$

It is important to note that the cytotoxic T-cell activation term b_A can either be facilitative and positive ($b_A \geq 0$) or inhibitory and negative ($b_A \leq 0$). Numerous experimental findings support this bimodality. For instance, these T-cells may get activated in response to fragments and debris from tumour cells, but may become suppressed in response to recurrent interactions with tumour cells. Let us now enter the corresponding substitutions from the aforementioned eqs. [(37)- (40)] have, into eq. (36), and then solve it for the r_{A2} weighting factor. We thereby can write the solution in compact form, as

$$G = \frac{r_{A1}}{\frac{\frac{b_A g_C}{C\left(1-\frac{\mu_C}{k_C}\right)} + b_A}{p_C A} - 1} \tag{41}$$

When we solve eq. 41 for r_{A2}, we get two values depending on the b_A value, which determines whether the cytotoxic T-cell activation is facilitative or inhibitory:

(a) If $b_A \leq 0$(T-cell inhibition): then one condition needs to be satisfied, viz. $r_{A2} \leq$G (42)

(b) If $b_A \geq 0$ (T-cell activation): then two conditions need to be satisfied, viz. $b_A \geq$ G (43)

$$\text{and } b_A < p_C A [1 + (r_{A1} / r_{A2})] \quad (44)$$

For using interleukin formation rate $v_C(t)$, we note that Eqs. (33 (a)), (42), (43) and (44) are the sufficient conditions on r_{A2}.

PART-B

Calculating the values of antitumour weights r_{M2} and r_{A2}

From the above, we have several numerical indices, viz. the parameters named (A, B, C, D, E, F, G) defined in eqs. (9 A), (14 A), (28), (33) and (41), and these indices determine the values that can be taken by the tuning parameters r_{M2} and r_{A2} [eqs.(10)-(11), (15)-(16), (27), (33 A), (42)-(43)]. The biological factors of eqs. (1)-(7) of chapter 2 [namely, (M, K, A, B, D, and C)] vary over time, so the values of r_{T2} and r_{A2} will also change over time.

Calculation of antitumour weight r_{M2}:

a) *When $b_M \leq 0$:*

The three aforesaid eqs.(10), (15), (27), respectively are:

$$A \leq r_{M2} < B;$$

$$C < r_{M2} \leq D;$$

$$r_{M_2} \leq E;$$

As D = ∞ (from eq. (14-A)), the last two of the above inequalities can be combined to get $C < r_{M2} \leq E$.

The two inequality formulas are now $A \leq r_{M2} < B$ and $C < r_{M2} \leq E$. Evidently, if we have a stricter inequality, we can satisfy both of these inequalities, that is:

[maximum of A and C] $\leq r_{M2} <$ [minimum B and E] (45)

As a starting point, we can consider the value of r_{M2} to be halfway between its upper and lower bounds, i.e. r_{M2} is average of the left- and right-sided expressions of eq. (45). Thus,

r_{M2} = ½ [(maximum of A and C) + (minimum of B and E)] (46)

Therefore, in the event that r_{M2} turns negative, we can take into account its upper bound in order to maintain a positive value. Thus, we can take

r_{M2} = ½ (minimum of B and E)] (47)

b) ***When the term $b_M \geq 0$:***

From eqs. (11), (16), and (27), we likewise arrive at the inequalities,

$A \geq r_{M2} > B$, and $C > r_{M2} \geq E$ (48)

Similarly,

r_{M2} = ½ [(the greater value among B and E) + (the smaller value among A and C)] (49)

If eq. (49) gives r_{M2} a negative value, then we take that

r_{M2} = ½ (the smaller value among A and C)] (50)

If this result is also negative, we shall not choose the antitumour inputes for r_{M2}, which are v_D(t), namely DAN impairment factor production rate and v_A(t), namily for tumour-infiltrating lymphocytes. Thus, the formation rate of the other two antitumour entities are omitted (or made zero), and only other antitumour entity, interlukin-2 is considered.

Calculation of antitumour weight r_{A2}:

a) ***When $b_L \leq 0$:***

From eqs. (33- A) and (42), we can get

$$r_{A2} = \text{G-1} \tag{51}$$

In case if (G-1) = F, then we have, (52)

$$r_{A2} = \text{G-2}$$

b) **When $b_L \geq 0$:**

By, eqs. (33-A), (43) and (44), one can discern that three conditions should be satisfied. We initially put

$$r_{A2} = \text{G+2} \tag{53}$$

In case, if eq. 44 inequality is not satisfying, we can put

$$r_{A2} = \text{G+1} \tag{54}$$

However, if r_{A2} + F, then, we can take

$$r_{A2} = \text{G+0.5} \tag{55}$$

PART-C

One or Two Antitumour entities

We can select the concentrations of the three antitumour entities based on the values of the weights, r_{M2} and r_{A2}, which depend on the values of bounds A, B, C, D, E, and F therein, as described in the earlier pages (Parts A and B, eqs. 9 A, 9 B, 14 A, 28, 33, 41). At first, we select all three antitumour entities. If any of the entities violates any of the necessary or sufficient conditions mentioned in aforesaid Part A and B, then we omit this entity and consider the other two antitumour entities. Following that, if one condition fails, the offending entity is omitted and we turn to the remaining antitumour entity. Below, we

explain how to proceed in a scenario where only one or two of the three antitumour modalities —DNA damage factor, T-cell, or IL-2 are required.

a) Formulation for two antitumour entities:

Due to the availability of the three different antitumour entities and owing to the simultaneous consideration of two entities out of the three, this strategy results in three distinct situations (namely T-cell and IL-2, or T-cell and DNA damage factor, or IL-2 and DNA damage factor). The aim is the same as with the three entities controls: to get the tumour cell population to $M = 0$ in a definite time t_F. Actually, we use the general strategy created for the full protocol of three medications in the derivations below. The following situation can occurs:

Case 1: DNA impairment with Tumour-infiltrating lymphocyte, ($v_D(t)$ and $v_A(t)$)

(i) Tumour cell module:

As, the previously defined tumour change rate is $M' = -\kappa_M(M - M^*)$, by using negative bias formulation, we have the following formulation of tumour cell extinction,

$$(\dot{M} - \dot{M}^*) + \kappa_M(M - M^*) = 0$$

This is similar to three antitumour entity control design. From eq. (17), we have the desired concentration of DNA blockage factor in blood ($D^{\ddagger}$) and the desired population of cytotoxic T-cells in blood ($A^{\ddagger}$) respectively as follows:

$$D^{\ddagger} = -ln(1 - U_D); \qquad \text{and} \qquad A^{\ddagger} = [s\, M^l\, U_A / (d - U_A)]^{1/l}$$

(ii) Cytotoxic T-cell module:

Similarly, for the dynamic control formulation of T-cell induced tumour regression:

$$(\dot{A} - \dot{A}^*) + \kappa_M(A - A^*) = 0$$

and the desired level of tumour-infiltrating lymphocyte formation is:

$$v_A(t) = -\left(f_A(X) + k_A(A - A^*) \right)$$

where, $f_A(X) = -mA + Aj[(Q^2M^2) / (k + Q^2M^2)] - qAM + (r_1K + r_2B)M - uKA^2 - k_A(1 - e^{-D})A$

(iii) DNA impairment factor module:

Similarly, the dynamic control formulation for DNA blockage factor-induced cancer regression is also obtained as:

$$(\dot{D} - \dot{D}^*) + \kappa_D(D - D^*) = 0$$

while the intended injection rate of tumours – infiltrate lymphocytes formation is:

$$v_D^{\ddagger} = \gamma D - k_D (D - D^{\ddagger})$$

Case 2: Tumour-infiltrating lymphocyte with Interleukin, ($v_A(t)$ and $v_I(t)$)

(i) Tumour cell module:

The formulation of cancer cell extinction with a negative bias is provided by the analysis mentioned in chapter 1:

$$(\dot{M} - \dot{M}^*) + \kappa_M(M - M^*) = 0$$

Also the efficacy factor of cytotoxic T-cell shown earlier, is:

$$U_M = \left(\frac{1}{M}\right)[\, aM(1 - bM) - cKM - K_M(1 - e^{-D})M + k_M(M - M^*)\,]$$

with the desired population of cytotoxic T-cell in blood having:

$$A^{\ddagger} = [s\, M^l\, U_A / (d - U_A)]^{1/l}$$

(ii) Cytotoxic T- cell module:

The aforesaid expressions we found are comparable to the three antitumour entities control strategies (described in Appendix- I), namely:

Efficacy factor of interleukin-2: $U_C = b_A / r_{A1} \, (1/ r_{A1} + 1/ r_{A2})$

Efficacy factor of tumour-infiltrating lymphocyte: $v_A = b_A / r_{A2} \mathrm{H}$ (where $\mathrm{H} = [1/ r_{A1} + 1/ r_{A2}]$)

Desired interleukin-2 concentration in blood: $C^{\ddagger} = g_C U_C / (p_C A - U_C)$

(iii) Interleukin module:

This is same as the three antitumour entities control systems, each of which has Interleukin-2 concentration rate that is desired:

$v_C^{\ddagger} = \mu_C C - k_C (C - C^{\ddagger})$

Case 3: Interleukin and DNA impairment factor, ($v_C(t)$ and $v_D(t)$)

(i) Tumour cell module:

As we discussed earlier, in chapter 2, the negative bias formulation for tumour cell elimination term is

$$(\dot{M} - \dot{M}^*) + \kappa_M (M - M^*) = 0$$

This is similar to the three antitumour entities control design, whereby we have

Desired DNA impairment factor concentration in blood: $D^{\ddagger} = -ln(1 - U_D)$;

Desired population of cytotoxic T-cells: $A^{\ddagger} = [s M^l U_A / (d - U_A)]^{1/l}$

(ii) Cytotoxic T- cell module:

Likewise, the T-cell induced tumour regression control dynamics can be represented by

$$(\dot{A} - \dot{A}^*) + \kappa_A(A - A^*) = 0$$

and the efficacy factor of interleukin-2 is

$$U_C = -[-mA + Aj[(Q^2M^2)/(k + Q^2M^2)] - qAM + (r_1K + r_2B)M - uKA^2 - k_A(1 - e^{-D})A$$

$$+ p_c AC/(g_C + C) + v_A(t) + \kappa_A(A - A^*)]$$

where the desired interleukin-2 concentration in the blood becomes:

$$C^{\ddagger} = g_C U_C/(p_C A - U_C)$$

(iii) DNA impairment factor module:

Reminiscent of the three antitumour entities control design earlier, we can obtain

Desired DNA impairment factor concentration in blood $v_D^{\ddagger}(t) = \gamma D - k_D(D - D^{\ddagger})$

(iv) Interleukin module:

As before, the desired interleukin-2 concentration in blood is, $v_C^{\ddagger} = \mu_C C - k_C(C - C^{\ddagger})$

b) Formulation for one antitumour entity:

Before moving on to one of the following three antitumour entities, we first discuss the dynamics of the tumour cell.

Case 1: DNA impairment factor module, $v_M(t)$

In this instance, the dynamics of the tumour cell and the contribution of the DNA blockage factor must be taken into account.

(i) Tumour cell module:

Here we have two modules to consider: the tumour cell modules, and its preceding module, the DNA blockage factor module (Figure 2.4). Following the same methodology, we can take

$$(\dot{M} - \dot{M}^*) + \kappa_M(M - M^*) = 0$$

Hence, the desired DNA blockage factor formulation in blood; $D^{\ddagger} = -ln(1 - U_D)$;

Here, the DNA blockage factor efficacy factor; $U_D = b_M / g_{MI}$

where, $g_{MI} = -k_M M$ and $b_M = -[\kappa_M(M - M^*) + f_M]$

and, $f_M = [aM(1 - bM) - cKM]$

(ii) DNA impairment factor module:

Recollecting the DNA impairment factor module of the three antitumour entities control design, we have the desired formulation rate of the DNA impairment factor:

$v_D^{\ddagger}(t) = \gamma D - k_D (D - D^{\ddagger})$

Case 2: Tumour-infiltrating lymphocyte formation rate, $v_A(t)$

In this case, we attend to the tumour cell module and its predecessor, the tumour infiltrating lymphocyte module (Figure 2.4).

(i) Tumour cell module:

Since we are dealing with immunomodulation, we consider the tumour cell module when under the immunomodulatory effect, namely the tumour infiltrating lymphocyte and interleukin-2, i.e. under the two antitumour entities formulation rates, $v_A(t)$ and $v_C(t)$. Thereby, we have the desired cytotoxic T-cell population in blood:

$$A^{\ddagger} = [s\, M^{l}\, U_A / (d - U_A)]^{1/l}$$

(ii) Cytotoxic T-cell module:

This resembles the cytotoxic T lymphocyte module under the effect of two antitumour entities, i.e. the formation rates of DNA impairment and tumour-infiltrating lymphocytes, i.e. the $v_M(t)$ and $v_A(t)$. Thus, the desired formation rate of tumour-infiltrating lymphocytes is:

$$v_A(t) = -\left(f_{LA}(X) + k_A(A - A^*)\right)$$

Case 3: Interleukin-2 formation rate, $v_C(t)$

Since the interleukin-2 dosage module $v_C(t)$, is most distant from the tumour cell module, we need to consider the three successive entities: tumour cell, cytotoxic T-cell and interleukin-2 module.

(i) Tumour cell module:

The derivation parallels the tumour cell module of the two antitumour entities, when formation rate of tumour-infiltrating lymphocytes and interleukin-2, $v_A(t)$ and $v_C(t)$, are used. Thence the desired cytotoxic T-cell population in blood is:

$$A^{\ddagger} = [s\, M^{l}\, U_A / (d - U_A)]^{1/l}$$

(ii) Cytotoxic T-cell module:

Here, also the derivation is same as the cytotoxic T-cell module of two the antitumour entities where one uses the formation rates of DNA impairment factor and interleukin-2, $v_D(t)$ and $v_C(t)$. Thereby the desired interleukin-2 concentration in blood is obtained as:

$$C^{\ddagger} = g_C\, U_C / (p_C A - U_C)$$

(iii) Interleukin-2 module:

This is reminiscent of the three antitumour entities administration; whereby the desired formation rate of interleukin-2 is:

$$v_C^{\ddagger} = \mu_C\, C - k_C\, (C - C^{\ddagger})$$

Following the procedures mentioned above, the one can determined the time-wise profile of the blood concentration of the antitumour entities and their formation rates of these entities. The individual concentration levels and formation rates vary with time, and this temporal profile of the antitumour entities (DNA blockage factor, Cytotoxic T- lymphocyte and Interleukin-2) drives the tumour cell population to extinction in the desired time duration.

APPENDIX – III (A)

Upregulated genes at time point t_1

Probe Set ID	Gene Name	Log FC	P.Value
Ssc.30843.1.A1_at	Q96LP2	5.09625862	2.5E-05
Ssc.13778.1.S1_at	IGHM	3.64518632	0.00483
Ssc.8843.1.A1_at	FN1	2.02799876	0.01463
Ssc.17853.1.A1_at	REM1	1.98507736	0.002
Ssc.19179.1.A1_at	NP_055654	1.9264786	0.02948
Ssc.27289.1.S1_at	GRIK2	1.86819834	0.00752
Ssc.11858.1.S1_at	FMOD	1.8643975	0.00603
Ssc.4258.1.S1_at	TP53I11	1.86029917	0.00178
Ssc.29707.1.A1_at	NP_115822	1.85472412	0.00139
Ssc.11698.1.A1_at	SIAT8D	1.76742182	0.00084
Ssc.25888.1.A1_at	NFIB	1.76622848	0.00261
Ssc.29185.1.A1_at	ITGA8	1.76621301	0.00432
Ssc.2070.1.S1_at	EPB41L1	1.76289291	7.5E-05
Ssc.8965.1.A1_at	EPAS1	1.75478446	0.01278
Ssc.2064.1.A1_at	Q86SM2	1.72424482	0.00022
Ssc.6656.1.A1_at	FNDC1	1.61675476	0.01466
Ssc.314.1.S1_at	ADM	1.57717706	0.01586
Ssc.30055.1.A1_at	RUNX1	1.51028593	0.02231
Ssc.24337.1.S1_at	MAPK9	1.4910113	0.032
Ssc.14422.1.A1_at	C6orf190	1.48253385	0.01322
Ssc.8569.1.A1_at	Q6NVV9	1.47638439	0.00279
Ssc.14164.1.A1_at	Q8N4P4	1.47420771	0.00605
Ssc.5631.1.S1_at	EPB41L1	1.45708193	0.00124
Ssc.9883.1.A1_at	ADRBK2	1.38293739	0.0007
Ssc.20491.1.A1_at	CLCN3	1.37308516	0.01877
Ssc.29372.1.A1_at	Q63HM9	1.37177953	0.04391
Ssc.27786.1.S1_at	PFKFB3	1.32202806	0.00407
Ssc.16187.1.S1_at	PTGDS	1.30616662	0.03569
Ssc.11992.1.A1_at	CLU	1.30234557	0.01724
Ssc.7907.1.A1_at	SIAT1	1.30015215	0.023
Ssc.18359.1.S1_at	CCR1	1.27669738	0.04576
Ssc.1600.1.A1_a_at	Q8N4P4	1.17748454	0.00552
Ssc.5910.1.A1_at	VAV1	1.16612458	0.0494
Ssc.16985.1.S1_at	IL18BP	1.13172202	0.01786
Ssc.11787.2.A1_at	RASSF2	1.13110809	0.02894

Ssc.5826.1.A1_at	CSF1R	1.12066561	0.02397
Ssc.15892.1.S1_at	KCNAB2	1.11647368	0.03449
Ssc.29929.1.S1_at	ANGPTL2	1.11116635	0.00757
Ssc.4520.1.S1_at	MYO1D	1.1066335	0.04137
Ssc.29026.1.S1_at	EPB41L1	1.09542659	0.00239
Ssc.15360.1.A1_a_at	SOX18	1.09371615	0.00883
Ssc.13825.1.A1_at	CABLES1	1.09085197	0.04619
Ssc.28019.1.A1_at	ATRNL1	1.07712333	0.01356
Ssc.1902.1.A1_at	Q8N200	1.05216308	0.04076
Ssc.4345.1.S1_at	COL4A1	1.05055533	0.00175
Ssc.2897.1.S1_at	CBLB	1.04402778	0.02037
Ssc.13356.1.A1_at	TKTL1	1.04160997	0.0076
Ssc.6365.1.A1_at	SYNE1	1.03083458	0.00371
Ssc.25203.1.S1_at	SCARA3	1.02684401	0.01165
Ssc.29504.1.A1_at	HYDIN	1.02434073	0.01694
Ssc.1017.1.S1_at	NP_056234	1.02069193	0.03923
Ssc.12790.1.A1_at	VEGFC	1.01248312	0.02595
Ssc.11440.1.A1_at	RCOR3	1.01151092	0.00027
Ssc.24733.1.A1_at	Q8IY15	1.01125332	0.01025

Downregulated genes at time point t_1

Probe Set ID	Gene Name	Log FC	P.Value
Ssc.1313.1.A1_at	NP_077001	-1.035	0.0004
Ssc.31207.1.S1_at	TMPO	-1.0655	0.01169
Ssc.21168.1.S1_at	HSPA14	-1.0841	3.5E-05
Ssc.9311.1.A1_at	PHLDA1	-1.1051	0.0048
Ssc.15824.1.S1_at	KPNA2	-1.1385	0.01054
Ssc.6430.1.A1_at	VAPB	-1.1477	0.02661
Ssc.24122.1.S1_at	KNTC2	-1.1592	0.0234
Ssc.8308.1.A1_at	CHL1	-1.1613	0.02133
Ssc.19649.2.S1_at	PSMD14	-1.2206	0.00022
Ssc.2045.2.S1_at	SLC23A3	-1.2472	0.00618
Ssc.6707.1.A1_at	GLDC	-1.2667	0.00152
Ssc.23877.1.S1_at	CCNA2	-1.3384	0.00524
Ssc.16088.1.S1_at	HMGCR	-1.3973	0.01116
Ssc.26386.2.S1_a_at	NP_057185	-1.4934	0.00177
Ssc.13665.1.A1_at	SCML2	-1.8469	0.00012
Ssc.20101.1.S1_at	G1P3	-2.2007	0.029

Upregulated genes at time point t_2

Probe Set ID	Gene Name	Log FC	P.Value
Ssc.13778.1.S1_at	IGHM	5.67482	0.00013
Ssc.30843.1.A1_at	Q96LP2	4.44237	0.00021
Ssc.19946.1.S1_at	IGLC1	4.05304	0.00152
Ssc.22164.1.S1_at	ATP6V0D2	4.04613	0.00016
Ssc.9914.1.A1_at	CKB	3.57454	6.1E-05
Ssc.14275.1.A1_at	Q96LP2	3.55771	0.00021
Ssc.5887.1.A1_at	Q96LP2	3.28737	0.00021
Ssc.8843.1.A1_at	FN1	2.89563	0.00162
Ssc.140.1.S1_at	AMBN	2.6721	0.00258
Ssc.575.1.S1_at	ACP5	2.5654	3.7E-05
Ssc.4520.1.S1_at	IGHM	2.51308	0.00013
Ssc.44.1.S1_at	ITGB3	2.50292	0.00815
Ssc.12774.1.A1_at	NP_940851	2.48555	7.9E-06
Ssc.14561.1.S1_at	ITGB2	2.46495	0.0008
Ssc.11075.3.S1_a_at	TVB1_HUMAN	2.45304	0.04079
Ssc.26709.1.S1_at	EBI2	2.4368	0.00203
Ssc.20177.1.S1_at	ITGB2	2.42692	0.0007
Ssc.11006.1.S1_at	SNX10	2.38426	5.4E-05
Ssc.13490.1.A1_at	STX7	2.35453	0.00445
Ssc.30761.1.A1_at	PSD4	2.33952	0.00147
Ssc.17853.1.A1_at	REM1	2.29709	0.00085
Ssc.24984.1.S1_at	ASAHL	2.2688	0.00461
Ssc.8965.1.A1_at	EPAS1	2.24248	0.00331
Ssc.508.1.S1_at	FCER1G	2.22444	0.00514
Ssc.5826.1.A1_at	Q96LP2	2.20903	0.00017
Ssc.12817.1.S1_at	PLXNA2	2.16675	0.00032
Ssc.22030.1.S1_at	CCL5	2.16659	0.03752
Ssc.18359.1.S1_at	CCR1	2.15474	0.00263
Ssc.507.1.A1_at	REM1	2.15086	0.00101
Ssc.11858.1.S1_at	FMOD	2.14319	0.00306
Ssc.5950.1.S1_at	DNM1	2.12712	0.01072
Ssc.5381.1.A1_at	COL27A1	2.08316	0.00648
Ssc.428.5.S1_at	TCA_HUMAN	2.08273	0.03386
Ssc.151.1.S1_at	CYBB	2.08116	0.01844
Ssc.26337.1.S1_at	PSD4	2.03985	0.00144
Ssc.20258.1.S1_at	Q8N4T3	1.99177	0.02489
Ssc.2187.1.S1_at	ITGB2	1.98419	0.00059
Ssc.11243.1.A1_at	KIF23	1.98418	0.00347
Ssc.4258.1.S1_at	TP53I11	1.98386	0.00154

Ssc.11992.1.A1_at	CLU	1.96924	0.00126
Ssc.16985.1.S1_at	IL18BP	1.92192	0.00045
Ssc.19359.2.S1_at	MBP	1.90985	0.02196
Ssc.2897.1.S1_at	CBLB	1.90635	0.00028
Ssc.23014.1.S1_at	ITGB2	1.90064	0.00061
Ssc.16769.1.S1_at	REM1	1.89839	0.00093
Ssc.18272.1.A1_at	SNX10	1.89206	5.3E-05
Ssc.15892.1.S1_at	KCNAB2	1.87578	0.00162
Ssc.10328.1.A1_at	NP_942123	1.87156	0.03843
Ssc.3621.1.S1_at	DPYSL3	1.86229	0.00485
Ssc.23804.1.S1_at	SLC7A3	1.85693	0.00612
Ssc.7907.1.A1_at	EPAS1	1.84462	0.0033
Ssc.21300.1.S1_at	PAPOLA	1.834	0.00235
Ssc.27790.1.A1_at	SNX10	1.80783	4.6E-05
Ssc.30598.1.A1_at	NRP2	1.79691	0.0004
Ssc.10931.1.S1_at	CRYAB	1.79059	0.02537
Ssc.30055.1.A1_at	RUNX1	1.78716	0.01116
Ssc.24337.1.S1_at	MAPK9	1.77316	0.01659
Ssc.15419.1.S1_at	BTK	1.76048	0.01466
Ssc.16186.1.S1_at	CD3E	1.7473	0.04381
Ssc.5.1.S1_a_at	CLECSF5	1.74678	0.03091
Ssc.16766.1.A1_at	DOK2	1.73921	0.00737
Ssc.19344.1.A1_at	RH25_HUMAN	1.73547	0.01022
Ssc.21570.1.S1_at	HEM1	1.72957	0.02251
Ssc.5287.1.S1_at	NP_443170	1.71689	0.00176
Ssc.5530.2.S1_at	ZNF205	1.71132	0.01243
Ssc.17159.1.S1_at	IMP1_HUMAN	1.70002	0.01392
Ssc.4283.1.S1_at	BIN2	1.69722	0.0048
Ssc.5910.1.A1_at	VAV1	1.69286	0.00888
Ssc.8594.1.A1_at	BLNK	1.68648	0.02122
Ssc.116.1.S1_at	GGT1	1.6733	0.00834
Ssc.19648.1.S1_at	PSD4	1.66602	0.00145
Ssc.16932.1.S1_at	CNOT2	1.65264	0.01106
Ssc.4792.1.A1_at	PRKCB1	1.64567	0.01288
Ssc.4779.1.A1_at	CPM	1.64452	0.00543
Ssc.9330.1.A1_at	LCP1	1.60983	0.00415
Ssc.19836.1.S1_at	SLC31A2	1.59581	0.03036
Ssc.26328.1.S1_at	CCR5	1.59068	0.0414
Ssc.16912.2.S1_at	Q9BY89	1.57954	0.02075
Ssc.3761.1.A1_at	C6orf103	1.57954	7.9E-05
Ssc.1902.1.A1_at	Q8N200	1.57659	0.00529
Ssc.6656.1.A1_at	FNDC1	1.56197	0.02311
Ssc.18135.1.S1_at	PRELP	1.55079	0.00604

Ssc.13176.1.S1_at	MBP	1.54071	0.02185
Ssc.14371.1.S1_at	MAP1A	1.53683	0.0151
Ssc.22037.2.S1_at	LAM5_HUMAN	1.53579	0.01787
Ssc.820.1.S1_at	ANPEP	1.53524	0.03397
Ssc.23516.1.S1_at	SATB1	1.53222	0.03505
Ssc.18425.1.S1_at	PTPRCAP	1.52611	0.02873
Ssc.15612.1.S1_at	PSD4	1.52553	0.0015
Ssc.7176.1.A1_at	CXCR4	1.52266	0.00496
Ssc.11787.2.A1_at	RASSF2	1.51281	0.00702
Ssc.9553.1.A1_s_at	NP_054778	1.50983	0.01409
Ssc.8063.1.A1_at	NP_061900	1.48693	0.0387
Ssc.13296.1.A1_at	FMOD	1.47149	0.00293
Ssc.6785.1.S1_at	LRP1	1.46053	0.01789
Ssc.8569.1.A1_at	STX7	1.45681	0.00445
Ssc.29504.1.A1_at	HYDIN	1.44748	0.00218
Ssc.18375.1.A1_at	SEMA4D	1.44001	0.01376
Ssc.2624.1.S1_at	Q8NHP8	1.43982	0.00168
Ssc.25839.1.S1_at	ECE2	1.43457	0.0109

Downregulated genes at time point t_2

Probe Set ID	Gene Name	Log FC	P.Value
Ssc.13499.1.A1_at	Q96KZ8	-1.00220	0.00041
Ssc.6789.2.S1_at	Q9BWC9	-1.01579	0.03728
Ssc.28128.1.A1_at	NRXN3	-1.02156	0.00533
Ssc.8308.1.A1_at	CHL1	-1.02159	0.04919
Ssc.14286.1.A1_at	C10orf78	-1.02896	0.00478
Ssc.25975.1.S1_at	HRMT1L3	-1.03380	0.00034
Ssc.7910.2.A1_a_at	HELLS	-1.03685	0.00318
Ssc.27652.1.A1_at	FAM33A	-1.04155	0.00033
Ssc.9434.1.A1_at	MARK1	-1.04393	0.02844
Ssc.10723.1.A1_at	FSHPRH1	-1.04575	0.00011
Ssc.29168.1.A1_at	PLA2G4A	-1.04817	0.00212
Ssc.5073.1.A1_at	EZH2	-1.05170	0.00354
Ssc.8180.1.A1_at	RFX4	-1.05615	0.04886
Ssc.22613.1.S1_at	Q7Z672	-1.06382	0.00036
Ssc.24916.1.S1_at	ESPL1	-1.07530	0.02052
Ssc.29056.1.S1_at	WDR43	-1.09256	0.01981
Ssc.18679.1.S1_at	TRIM59	-1.10309	0.00378
Ssc.13526.1.A1_at	C10orf64	-1.10761	0.00096
Ssc.13295.1.A1_at	SNX25	-1.10884	0.01226
Ssc.9387.2.S1_at	PCNA	-1.10960	0.00231

Ssc.26779.1.A1_at	CDH17	-1.11128	0.00020
Ssc.26662.1.S1_at	Q9H989	-1.11787	0.00777
Ssc.27995.1.A1_at	UHRF1	-1.12336	0.01472
Ssc.1408.2.S1_at	MCM2	-1.12336	0.00706
Ssc.17900.1.S1_at	C6orf162	-1.12745	0.00182
Ssc.4612.1.S1_at	MCM4	-1.12801	0.00435
Ssc.7153.1.A1_at	NASP	-1.13065	0.00190
Ssc.29706.1.A1_at	NP_054828	-1.13686	0.01381
Ssc.19940.1.S1_at	CCDC5	-1.14127	0.00002
Ssc.7202.1.A1_at	MCM6	-1.14339	0.00095
Ssc.4403.1.A1_at	CKS1B	-1.14902	0.00003
Ssc.16363.1.S1_at	TMOD3	-1.14961	0.02086
Ssc.16088.1.S1_at	HMGCR	-1.15409	0.03971
Ssc.24195.1.A1_at	ARHGAP19	-1.16515	0.00021
Ssc.24459.1.S1_at	NP_057532	-1.16660	0.01287
Ssc.24353.1.S1_at	VRK1	-1.17160	0.00103
Ssc.21974.2.S1_a_at	OSGEP	-1.18067	0.00040
Ssc.6654.1.A1_at	ACSL3	-1.18730	0.03462
Ssc.19205.1.A1_at	C7orf24	-1.18903	0.00018
Ssc.6338.2.S1_at	USP1	-1.18982	0.00106
Ssc.9311.1.A1_at	PHLDA1	-1.19071	0.00394
Ssc.24505.1.A1_at	DZIP1	-1.21352	0.00410
Ssc.13476.1.A1_at	Q86TG7	-1.21378	0.04162
Ssc.29650.1.A1_at	CHEK1	-1.22007	0.00055
Ssc.31027.1.A1_at	KIAA1333	-1.23674	0.00033
Ssc.226.1.S1_at	HMGB2	-1.23874	0.00113
Ssc.2045.2.S1_at	SLC23A3	-1.24221	0.00875
Ssc.11477.1.S1_at	IMMP2L	-1.24364	0.00139
Ssc.5721.1.S1_at	CDC45L	-1.25383	0.00307
Ssc.23207.1.S1_at	RNF2	-1.25694	0.00335
Ssc.25336.1.S1_at	KIAA1430	-1.26113	0.00592
Ssc.9387.1.A1_at	PCNA	-1.26415	0.00318
Ssc.18136.1.A1_at	NP_079143	-1.28426	0.00256
Ssc.18907.1.A1_at	DNA2L	-1.29992	0.00013
Ssc.26386.2.S1_a_at	NP_057185	-1.31685	0.00665
Ssc.19205.2.S1_at	C7orf24	-1.32061	0.00023
Ssc.19675.1.S1_at	RACGAP1	-1.32262	0.00100
Ssc.16931.1.S1_at	CCNB3	-1.33225	0.00019
Ssc.11984.1.A1_at	FANCD2	-1.33242	0.00030
Ssc.5983.1.A1_at	Q9NSG2	-1.34550	0.00063
Ssc.10642.1.S1_at	CTNNA3	-1.36346	0.00371
Ssc.11264.1.A1_at	TOM1L2	-1.36881	0.00098
Ssc.27353.1.A1_at	CHAF1B	-1.37224	0.00088

Ssc.29094.1.A1_at	ECT2	-1.37457	0.00046
Ssc.7139.1.S1_at	DHFR	-1.38693	0.00045
Ssc.2712.1.S1_at	NP_055544	-1.39243	0.00551
Ssc.7546.1.A1_at	NP_955389	-1.39759	0.00007
Ssc.11164.2.S1_a_at	Q96JN1	-1.40730	0.00274
Ssc.31026.1.A1_at	Q86T96	-1.42889	0.00226
Ssc.20770.1.S1_at	NSD1	-1.43943	0.00215
Ssc.23877.2.A1_at	CCNA2	-1.43989	0.00055
Ssc.21605.2.S1_at	NUSAP1	-1.44307	0.00030
Ssc.11630.1.S1_at	PTTG2	-1.44755	0.00076
Ssc.24094.1.S1_at	Q9BSJ6	-1.45046	0.00966
Ssc.21605.1.S1_a_at	NUSAP1	-1.45132	0.00136
Ssc.27540.2.S1_at	UBE2C	-1.45271	0.00367
Ssc.2953.1.A1_at	C21orf45	-1.47204	0.00074
Ssc.7517.1.A1_at	Q8N340	-1.47823	0.00896
Ssc.21611.1.S1_at	TRPC5	-1.49554	0.00184
Ssc.5129.1.S1_at	MAD2L1	-1.50154	0.00010
Ssc.26753.1.A1_at	CACNA2D1	-1.51881	0.01843
Ssc.12493.1.A1_at	PAFAH1B2	-1.52289	0.00012
Ssc.7621.1.A1_at	ANLN	-1.53097	0.00327
Ssc.432.1.S1_at	BIRC5	-1.53222	0.00350
Ssc.18205.1.S1_at	Q9BSD3	-1.54181	0.00020
Ssc.5401.1.S1_at	Q14691	-1.54897	0.00147
Ssc.15824.1.S1_at	KPNA2	-1.55768	0.00147
Ssc.27206.1.A1_at	RAB6B	-1.56919	0.02162
Ssc.2754.1.S1_at	PRC1	-1.56951	0.00235
Ssc.25215.1.A1_at	PLK4	-1.59078	0.00011
Ssc.7190.1.S1_at	BUB1B	-1.60832	0.00092
Ssc.5371.3.S1_a_at	POLE2	-1.65905	0.00091
Ssc.2154.3.S1_a_at	KIF2C	-1.67045	0.00245
Ssc.17991.1.A1_at	Q6ZN37	-1.67705	0.00257
Ssc.11879.1.A1_at	CDC6	-1.68145	0.00288
Ssc.7218.1.A1_at	KIAA0101	-1.68248	0.00138
Ssc.13876.1.S1_at	NEK2	-1.68422	0.00346
Ssc.2224.1.S1_at	CENPF	-1.69221	0.00194
Ssc.27717.1.S1_at	CDK11	-1.70528	0.00079
Ssc.5721.3.S1_a_at	CDC45L	-1.72445	0.00144

Upregulated genes at time point t_3

Probe Set ID	Gene Name	Log FC	P.Value
Ssc.14275.1.A1_at	CALCR	7.12082	0.00000
Ssc.13778.1.S1_at	IGHM	6.91222	0.00001
Ssc.22164.1.S1_at	ATP6V0D2	6.21724	0.00000
Ssc.30843.1.A1_at	Q96LP2	6.06362	0.00000
Ssc.9914.1.A1_at	CKB	5.19846	0.00000
Ssc.19946.1.S1_at	IGLC1	4.88860	0.00026
Ssc.44.1.S1_at	ITGB3	4.76798	0.00002
Ssc.5.1.S1_a_at	CLECSF5	4.71424	0.00000
Ssc.4520.1.S1_at	MYO1D	4.60638	0.00000
Ssc.26709.1.S1_at	EBI2	4.55933	0.00000
Ssc.27790.1.A1_at	SIGLEC5	4.54622	0.00000
Ssc.13490.1.A1_at	STX7	4.49171	0.00001
Ssc.8843.1.A1_at	FN1	4.47863	0.00002
Ssc.20258.1.S1_at	Q8N4T3	4.43314	0.00003
Ssc.10328.1.A1_at	NP_942123	4.35451	0.00005
Ssc.30059.1.A1_at	NP_115724	4.33218	0.00006
Ssc.24984.1.S1_at	ASAHL	4.31292	0.00001
Ssc.116.1.S1_at	GGT1	4.24825	0.00000
Ssc.6656.1.A1_at	FNDC1	4.15442	0.00000
Ssc.140.1.S1_at	AMBN	4.03418	0.00004
Ssc.4128.1.A1_at	PDE4DIP	4.02149	0.00000
Ssc.11006.1.S1_at	SNX10	3.98494	0.00000
Ssc.20177.1.S1_at	SPI1	3.97537	0.00000
Ssc.4258.1.S1_at	TP53I11	3.97340	0.00000
Ssc.16640.1.A1_at	NP_009199	3.96374	0.00122
Ssc.17853.1.A1_at	REM1	3.95911	0.00000
Ssc.18011.1.S1_at	POPDC3	3.94528	0.00010
Ssc.5950.1.S1_at	DNM1	3.93491	0.00004
Ssc.2187.1.S1_at	CUTL2	3.92843	0.00000
Ssc.14561.1.S1_at	ITGB2	3.89810	0.00000
Ssc.19836.1.S1_at	SLC31A2	3.86734	0.00001
Ssc.12128.1.A1_at	NP_940851	3.85855	0.00000
Ssc.30761.1.A1_at	PSD4	3.84103	0.00001
Ssc.26200.1.S1_at	THRB	3.82928	0.00000
Ssc.820.1.S1_at	ANPEP	3.82149	0.00001
Ssc.12817.1.S1_at	PLXNA2	3.80896	0.00000
Ssc.6765.1.S1_at	SCIN	3.80222	0.00024
Ssc.11858.1.S1_at	FMOD	3.78240	0.00001
Ssc.8261.1.A1_at	CYP2C9	3.77004	0.00051

Ssc.9362.1.A1_at	COL1A2	3.73702	0.00001
Ssc.5381.1.A1_at	COL27A1	3.70662	0.00003
Ssc.18359.1.S1_at	CCR1	3.68305	0.00001
Ssc.5826.1.A1_at	CSF1R	3.68300	0.00000
Ssc.11243.1.A1_at	KIF23	3.66408	0.00001
Ssc.11992.1.A1_at	CLU	3.64200	0.00000
Ssc.508.1.S1_at	FCER1G	3.61783	0.00005
Ssc.19359.1.A1_at	MBP	3.60163	0.00001
Ssc.5287.1.S1_at	NP_443170	3.60006	0.00000
Ssc.4283.1.S1_at	BIN2	3.59273	0.00000
Ssc.18895.1.A1_at	FAM40B	3.56091	0.00000
Ssc.11075.3.S1_a_at	TVB1_HUMAN	3.54770	0.00485
Ssc.507.1.A1_at	TYROBP	3.53415	0.00000
Ssc.4511.1.S1_at	DHRS3	3.51406	0.00013
Ssc.16912.1.S1_at	Q9BY89	3.50529	0.00000
Ssc.4779.1.A1_at	CPM	3.49541	0.00000
Ssc.2897.1.S1_at	CBLB	3.49086	0.00000
Ssc.10931.1.S1_at	CRYAB	3.47941	0.00013
Ssc.16218.1.S1_at	ITGA2	3.46512	0.00000
Ssc.575.1.S1_at	ACP5	3.44830	0.00000
SscAffx.21.1.S1_at	CYP7A1	3.44291	0.00000
Ssc.8965.1.A1_at	EPAS1	3.42390	0.00005
Ssc.8594.1.A1_at	BLNK	3.42108	0.00006
Ssc.30055.1.A1_at	RUNX1	3.41994	0.00003
Ssc.26893.1.A1_at	NP_114141	3.41533	0.00019
Ssc.15419.1.S1_at	BTK	3.39813	0.00005
Ssc.27201.1.S1_a_at	CCRL2	3.38752	0.00028
Ssc.26337.1.S1_at	ICAM2	3.36781	0.00001
Ssc.19688.1.S1_at	CHRNA1	3.36575	0.00015
Ssc.20133.1.A1_at	THY1	3.36271	0.00000
Ssc.16234.1.S1_at	TCN1	3.36206	0.00233
Ssc.27360.1.A1_at	TIAM1	3.34197	0.00110
Ssc.26060.1.A1_at	MAFB	3.32355	0.00004
Ssc.15378.1.A1_at	NP_078993	3.31854	0.00001
Ssc.29185.1.A1_at	ITGA8	3.31755	0.00001
Ssc.7176.1.A1_at	CXCR4	3.31679	0.00000
Ssc.21537.1.A1_at	PARVB	3.29538	0.00000
Ssc.4466.1.S1_at	TEC	3.29374	0.00000
Ssc.428.5.S1_at	TCA_HUMAN	3.28569	0.00179
Ssc.25888.1.A1_at	NFIB	3.28243	0.00001
Ssc.23516.1.S1_at	SATB1	3.27466	0.00010
Ssc.19364.1.S1_at	C2	3.25614	0.00054
Ssc.2624.2.S1_at	Q8NHP8	3.25565	0.00000

Ssc.16494.1.A1_at	DOK3	3.24516	0.00000
Ssc.24337.1.S1_at	MAPK9	3.23972	0.00011
Ssc.18272.1.A1_at	TCIRG1	3.23452	0.00000
Ssc.18504.1.S1_at	DSCR1L1	3.19751	0.00000
Ssc.8647.1.A1_at	DISC1	3.17952	0.00001
Ssc.12138.1.A1_at	ROBO1	3.17779	0.00005
Ssc.23770.1.S1_at	ARSB	3.16857	0.00000
Ssc.151.1.S1_at	CYBB	3.16388	0.00087
Ssc.1526.1.S1_at	Q8N2F5	3.16283	0.00003
Ssc.18375.1.A1_at	SEMA4D	3.16044	0.00001
Ssc.23834.1.S1_at	SUSD3	3.15697	0.00001
Ssc.18343.1.A1_at	NP_938203	3.15546	0.00008
Ssc.19344.1.A1_at	RH25_HUMAN	3.15526	0.00005
Ssc.9330.1.A1_at	LCP1	3.13755	0.00000
Ssc.21091.1.S1_at	MYO1F	3.12812	0.00005
Ssc.20917.1.S1_at	C5orf13	3.12520	0.00004
Ssc.26328.1.S1_at	CCR5	3.12272	0.00036
Ssc.30598.1.A1_at	NRP2	3.10583	0.00000

Downregulated genes at time point t_3

Probe Set ID	Gene Name	Log FC	P.Value
Ssc.15257.1.S1_a_at	ACE2	-1.00045	0.00033
Ssc.21124.1.S1_at	O43328	-1.00680	0.00020
Ssc.30633.1.S1_at	NP_060835	-1.00814	0.00081
Ssc.28023.1.A1_at	ZNF521	-1.01111	0.00034
Ssc.17250.1.S1_at	QDPR	-1.01119	0.00164
Ssc.11012.1.A1_at	MSRB_HUMAN	-1.01343	0.01673
Ssc.25151.1.S1_at	C6orf79	-1.01384	0.00010
Ssc.13593.1.A1_at	Q9C0F7	-1.01527	0.00001
Ssc.8143.1.A1_at	RAPGEF2	-1.01600	0.00034
Ssc.25216.1.S1_at	PLCZ1	-1.01808	0.00003
Ssc.9439.1.A1_a_at	FUBP1	-1.01954	0.00002
Ssc.1705.1.S1_at	PCBD	-1.02035	0.00613
Ssc.7523.1.A1_at	PHB	-1.02119	0.00036
Ssc.24392.1.S1_at	RAB5B	-1.02239	0.01602
Ssc.30944.1.A1_at	MRE11A	-1.02370	0.00248
Ssc.3998.1.S1_at	Q96EY4	-1.02897	0.00032
Ssc.2505.2.S1_at	AKAP11	-1.03112	0.00204
Ssc.8819.1.A1_at	HPS3	-1.03190	0.00464
Ssc.3249.1.S1_at	QSCN6	-1.03274	0.00390
Ssc.24918.1.S1_at	Q9P2K6	-1.03354	0.00236

Ssc.22204.2.A1_at	PIP3AP	-1.03447	0.00002
Ssc.7413.1.A1_at	DNMT3B	-1.03590	0.00000
Ssc.14573.1.S1_at	EYA2	-1.03599	0.00021
Ssc.7281.2.A1_at	SFRS10	-1.03676	0.00000
Ssc.22547.1.S1_at	TTF2	-1.03792	0.00034
Ssc.21547.1.A1_at	Q9UI58	-1.03977	0.00328
Ssc.5517.1.A1_at	MAP3K12	-1.04156	0.00116
Ssc.7446.1.S1_a_at	PPID	-1.04179	0.00000
Ssc.22824.1.S1_at	SEPHS1	-1.04246	0.00042
Ssc.3091.1.A1_at	HECA	-1.04322	0.00038
Ssc.4482.2.S1_at	PPP2R5C	-1.04560	0.00575
Ssc.7221.1.S1_at	H2AFV	-1.04633	0.00000
Ssc.19103.1.A1_at	MED8	-1.04725	0.00123
Ssc.30818.1.S1_at	NUFIP1	-1.04955	0.00023
Ssc.25561.1.A1_at	PWP1_HUMAN	-1.04965	0.00005
Ssc.5220.1.S1_at	SFRS9	-1.05033	0.00002
Ssc.10395.1.A1_at	TAF9	-1.05271	0.00005
Ssc.3952.1.S1_at	SAE2_HUMAN	-1.05353	0.00000
Ssc.1006.1.S1_at	PGM1	-1.05431	0.00101
Ssc.11700.1.A1_at	SERAC1	-1.05557	0.00019
Ssc.25535.1.S1_at	TM6SF1	-1.05564	0.00035
Ssc.6448.1.S1_at	Q6GMV3	-1.05675	0.00011
Ssc.27880.1.S1_at	BID	-1.05842	0.00005
Ssc.5524.1.S1_at	C1orf24	-1.05843	0.00270
Ssc.4556.1.S1_at	NUP107	-1.05918	0.00009
Ssc.17027.1.S1_at	ATAD3A	-1.05926	0.00012
Ssc.1449.1.S1_at	SMC1L1	-1.06420	0.00002
Ssc.5300.1.S1_at	NP_060209	-1.06534	0.00108
Ssc.5638.1.S1_at	FKBP4	-1.06634	0.00035
Ssc.8379.1.A1_at	SLC35A1	-1.06705	0.00010
Ssc.6423.1.A1_at	KIAA0934	-1.06867	0.04689
Ssc.31040.1.A1_at	CC4L_HUMAN	-1.07230	0.00016
Ssc.2879.1.S1_at	SLC25A25	-1.07353	0.00449
Ssc.25399.1.S1_at	FBXL11	-1.07519	0.00000
Ssc.8274.1.A1_at	PFN2	-1.07522	0.01618
Ssc.1398.1.S1_at	KCTD15	-1.07742	0.00069
Ssc.9450.1.S1_at	MYLK	-1.07794	0.00791
Ssc.3772.1.A1_at	SGCE	-1.07888	0.00103
Ssc.1632.1.S1_at	DKKL1	-1.08325	0.00116
Ssc.26113.2.S1_at	Q9H6L5	-1.08332	0.02777
Ssc.10928.1.A1_at	PCTK2	-1.08640	0.00079
Ssc.10918.1.A1_at	NP_057142	-1.08792	0.00002
Ssc.1210.1.A1_at	C14orf130	-1.08914	0.00001

Ssc.12091.1.A1_at	SMARCA1	-1.09155	0.00396
Ssc.17872.1.A1_at	NR2F1	-1.09463	0.01696
Ssc.24250.1.S1_at	CRABP2	-1.09700	0.01425
Ssc.5008.1.A1_at	GSTA4	-1.09803	0.00033
Ssc.7735.2.S1_at	ARPC1A	-1.10072	0.00005
Ssc.16964.2.S1_a_at	C13orf11	-1.10481	0.00029
Ssc.21545.1.S1_at	PCNX	-1.10491	0.00294
Ssc.24422.1.S1_at	UBE2S	-1.10576	0.00008
Ssc.9819.1.S1_at	PGRMC1	-1.10716	0.00188
Ssc.12709.1.A1_at	LMNB2	-1.10987	0.00003
Ssc.10723.1.A1_at	FSHPRH1	-1.11069	0.00005
Ssc.21205.1.S1_at	MRPL19	-1.11114	0.00008
Ssc.24710.1.S1_at	Q8IYR3	-1.11164	0.00225
Ssc.18474.1.S1_at	EIF2B3	-1.11444	0.00004
Ssc.5105.2.S1_a_at	GPRC5B	-1.11681	0.00229
Ssc.20772.1.S1_at	USP39	-1.11988	0.00010
Ssc.6371.1.A1_at	PRNP	-1.12016	0.00237
Ssc.16861.1.A1_at	Q8N221	-1.12041	0.00006
Ssc.12888.1.S1_at	WRB	-1.12422	0.00012
Ssc.7797.1.S1_at	TMED8	-1.13034	0.00008
Ssc.8408.1.A1_at	Q8N815	-1.13154	0.00005
Ssc.3313.1.S1_at	HSPA4	-1.13164	0.00004
Ssc.30936.1.S1_at	ACTR8	-1.13396	0.00025
Ssc.24084.1.A1_at	ACVR2B	-1.13500	0.00646
Ssc.21701.1.S1_at	FEN1	-1.13571	0.00014
Ssc.8905.1.A1_at	NP_976224	-1.13698	0.00219
Ssc.19940.1.S1_at	CCDC5	-1.13747	0.00002
Ssc.22216.1.A1_at	RBBP8	-1.13792	0.00001
Ssc.29410.1.A1_at	PLCB4	-1.13979	0.04825
Ssc.12312.1.A1_at	NOLC1	-1.14097	0.00002
Ssc.12335.2.S1_a_at	Q8WVE0	-1.14217	0.00009
Ssc.18635.1.S1_at	SIVA_HUMAN	-1.14474	0.00004
Ssc.17330.2.A1_at	C10orf86	-1.14687	0.00000
Ssc.7694.1.A1_at	TOPBP1	-1.14717	0.00000
Ssc.20481.1.A1_at	KIAA0020	-1.14773	0.00003
Ssc.18475.2.S1_at	PTE2_HUMAN	-1.14848	0.00002
Ssc.18475.3.A1_at	NP_689544	-1.15136	0.00187

Upregulated genes at time point t_4

Probe Set ID	Gene Name	logFC	P.Value
Ssc.13778.1.S1_at	IGHM	8.89414	0.00000
Ssc.21582.1.S1_at	UBD	7.60756	0.00013
Ssc.15871.1.S1_a_at	KLRC4	7.16283	0.00000
Ssc.19946.1.S1_at	IGLC1	6.68796	0.00004
Ssc.11075.1.S1_a_at	TVB1_HUMAN	6.52247	0.00003
Ssc.11208.1.S1_at	0	6.51235	0.00001
Ssc.140.1.S1_at	AMBN	5.87610	0.00000
Ssc.19640.1.A1_at	FCER1A	5.83251	0.00005
Ssc.19364.1.S1_at	C2	5.73833	0.00000
Ssc.428.5.S1_at	TCA_HUMAN	5.61810	0.00004
Ssc.22030.1.S1_at	CCL5	5.57566	0.00008
Ssc.8261.1.A1_at	CYP2C9	5.46767	0.00005
Ssc.18610.1.A1_at	NEBL	5.41186	0.00002
Ssc.23793.1.S1_at	CD2	5.28899	0.00010
Ssc.5.1.S1_a_at	CLECSF5	5.11144	0.00001
Ssc.30843.1.A1_at	Q96LP2	4.83335	0.00044
Ssc.16234.1.S1_at	TCN1	4.82567	0.00036
Ssc.6765.1.S1_at	SCIN	4.81311	0.00010
Ssc.16186.1.S1_at	CD3E	4.69962	0.00007
Ssc.5614.1.S1_at	TPS1	4.64796	0.00001
Ssc.20832.1.S1_at	SCTR	4.57076	0.00000
Ssc.12825.1.A1_at	NP_742001	4.55931	0.00029
Ssc.22164.1.S1_at	ATP6V0D2	4.51310	0.00025
Ssc.18010.1.A1_at	SH2D1A	4.46911	0.00011
Ssc.27201.1.S1_a_at	CCRL2	4.45950	0.00007
Ssc.14561.1.S1_at	ITGB2	4.44710	0.00001
Ssc.180.1.S1_at	TRGV9	4.41453	0.00001
Ssc.19619.1.S1_at	LCK	4.39025	0.00010
Ssc.26328.1.S1_at	CCR5	4.38560	0.00005
Ssc.20294.1.S1_at	Q8N8D9	4.38410	0.00006
Ssc.26709.1.S1_at	EBI2	4.22750	0.00004
Ssc.9362.1.A1_at	COL1A2	4.17361	0.00002
Ssc.16640.3.S1_at	NP_009199	4.17299	0.00007
Ssc.151.1.S1_at	CYBB	4.14623	0.00028
Ssc.1813.1.S1_at	PRODH	4.12558	0.00016
Ssc.7907.1.A1_at	SIAT1	4.00587	0.00000
Ssc.23804.1.S1_at	SLC7A3	3.99738	0.00001
Ssc.26300.2.S1_at	UNC93B1	3.99558	0.00001
Ssc.508.1.S1_at	FCER1G	3.97477	0.00010

Ssc.18938.1.A1_at	CPZ	3.95943	0.00010
Ssc.20177.1.S1_at	SPI1	3.94920	0.00002
Ssc.10346.1.A1_at	HEM1	3.94679	0.00003
Ssc.8594.1.A1_at	BLNK	3.94662	0.00006
Ssc.11006.1.S1_at	SNX10	3.93449	0.00000
Ssc.1206.1.A1_at	ADAMTS19	3.91519	0.00000
Ssc.16932.1.S1_at	CNOT2	3.91097	0.00001
Ssc.709.1.S1_at	GLRX	3.90162	0.00001
Ssc.24944.1.S1_a_at	FCGR1A	3.89952	0.00002
Ssc.30761.1.A1_at	PSD4	3.87304	0.00004
Ssc.3285.1.S1_at	ST14	3.87261	0.00079
Ssc.19980.1.S1_at	ADAM28	3.85575	0.00000
Ssc.5381.1.A1_at	COL27A1	3.85434	0.00010
Ssc.22620.1.S1_at	IFIT2	3.85133	0.00000
Ssc.30059.1.A1_at	NP_115724	3.83423	0.00108
Ssc.15419.1.S1_at	BTK	3.81262	0.00007
Ssc.16766.1.A1_at	DOK2	3.77573	0.00002
Ssc.5108.1.S1_at	C9	3.73134	0.00001
Ssc.26337.1.S1_at	ICAM2	3.72783	0.00001
Ssc.19344.1.A1_at	RH25_HUMAN	3.72574	0.00004
Ssc.18425.1.S1_at	PTPRCAP	3.69418	0.00009
Ssc.30637.1.A1_at	SLC39A11	3.66455	0.00015
Ssc.21091.1.S1_at	MYO1F	3.61720	0.00006
Ssc.24337.1.S1_at	MAPK9	3.61195	0.00018
Ssc.7275.1.S1_at	KYNU	3.58998	0.00000
Ssc.19648.1.S1_at	SLC15A3	3.58735	0.00000
Ssc.20464.1.S1_at	GLIPR1	3.58009	0.00004
Ssc.5910.1.A1_at	VAV1	3.57831	0.00004
Ssc.11025.1.S1_at	HLA-DMB	3.57467	0.00004
Ssc.16494.1.A1_at	DOK3	3.57460	0.00000
Ssc.24984.1.S1_at	ASAHL	3.57174	0.00034
Ssc.30602.1.A1_at	Q6ZRW2	3.57052	0.00004
Ssc.20113.1.S1_at	FRMD4B	3.55606	0.00188
Ssc.507.1.A1_at	TYROBP	3.54949	0.00002
Ssc.17297.1.A1_at	CLIC2	3.53255	0.00003
Ssc.4792.1.A1_at	PRKCB1	3.52186	0.00007
Ssc.18359.1.S1_at	CCR1	3.51833	0.00011
Ssc.14475.3.S1_a_at	PPARG	3.50459	0.00002
Ssc.6055.1.A1_at	Q6P9B3	3.49603	0.00015
Ssc.12682.1.A1_at	VAV3	3.48311	0.00016
Ssc.2140.1.S1_at	PTK2B	3.48011	0.00001
Ssc.31189.1.S1_at	CHPT1	3.47867	0.00007
Ssc.19359.1.A1_at	MBP	3.46705	0.00011

Ssc.13176.1.S1_at	CORO1A	3.46291	0.00011
Ssc.114.1.S1_at	HSPA6	3.44387	0.00001
Ssc.7969.1.A1_at	POSTN	3.43792	0.00227
Ssc.12138.1.A1_at	ROBO1	3.41678	0.00012
Ssc.5887.1.A1_at	SLC37A2	3.41566	0.00068
Ssc.3541.1.A1_at	NOSTRIN	3.41351	0.00000
Ssc.10931.1.S1_at	CRYAB	3.39479	0.00083
Ssc.7176.1.A1_at	CXCR4	3.36796	0.00001
Ssc.26200.1.S1_at	THRB	3.36577	0.00011
Ssc.314.1.S1_at	ADM	3.36349	0.00017
Ssc.29232.1.A1_at	SLC1A2	3.35987	0.00000
Ssc.1138.1.A1_at	LAMA2	3.35428	0.00006
Ssc.23516.1.S1_at	SATB1	3.34622	0.00040
Ssc.27360.1.A1_at	TIAM1	3.34265	0.00393
Ssc.26060.1.A1_at	MAFB	3.33947	0.00022
Ssc.2624.2.S1_at	Q8NHP8	3.31838	0.00000
Ssc.20101.1.S1_at	G1P3	3.31672	0.00892
Ssc.8854.1.A1_at	ARHGAP27	3.31671	0.00060

Downregulated genes at time point t_4

Probe Set ID	Gene Name	Log FC	P.Value
Ssc.8220.1.A2_at	RNPC2	-1.0004	0.0000
Ssc.21965.1.S1_at	NUP35	-1.0011	0.0005
Ssc.8732.1.A1_at	SLK	-1.0017	0.0005
Ssc.1559.1.S1_at	Q9BV81	-1.0025	0.0000
Ssc.2719.1.A1_at	MTA3	-1.0041	0.0008
Ssc.7442.1.A1_at	Q8N4K7	-1.0098	0.0000
Ssc.1648.1.S1_at	CTNND1	-1.0104	0.0001
Ssc.3608.1.S1_at	PTDSS2	-1.0164	0.0007
Ssc.26172.1.S1_at	NO55_HUMAN	-1.0171	0.0002
Ssc.18447.1.S1_at	SCAMP5	-1.0172	0.0017
Ssc.23999.1.S1_a_at	WDHD1	-1.0228	0.0025
Ssc.5792.1.S1_at	CTNNA1	-1.0232	0.0002
Ssc.7919.1.A1_at	PMS1	-1.0245	0.0029
Ssc.13526.1.A1_at	C10orf64	-1.0254	0.0062
Ssc.24702.1.S1_at	Q5T4D3	-1.0261	0.0001
Ssc.26671.1.A1_at	KIAA1704	-1.0292	0.0071
Ssc.9241.1.A1_at	SFRS6	-1.0293	0.0010
Ssc.23897.1.S1_a_at	CENTG2	-1.0314	0.0001

Ssc.5998.1.S1_at	Q9BTE6	-1.0343	0.0000
Ssc.11748.1.S1_at	PHLDB1	-1.0352	0.0019
Ssc.5073.1.A1_at	EZH2	-1.0359	0.0114
Ssc.24344.1.S1_a_at	DNMT1	-1.0365	0.0010
Ssc.1301.1.S1_at	HADH2	-1.0368	0.0001
Ssc.25792.1.S1_at	DSCR5	-1.0376	0.0014
Ssc.5664.1.S1_at	IHPK2	-1.0385	0.0002
Ssc.7929.1.A1_at	TBC1D15	-1.0395	0.0029
Ssc.8379.1.A1_at	SLC35A1	-1.0406	0.0006
Ssc.21880.1.S1_at	KIAA1166	-1.0466	0.0010
Ssc.26767.1.S1_at	ZFPM2	-1.0498	0.0222
Ssc.10394.1.A1_at	RBM8A	-1.0529	0.0000
Ssc.1814.1.S1_at	TIMM17B	-1.0545	0.0001
Ssc.29026.1.S1_at	EPB41L1	-1.0583	0.0127
Ssc.6887.1.S1_at	HNRPDL	-1.0594	0.0000
Ssc.12984.1.A1_s_at	C13orf9	-1.0594	0.0000
Ssc.29959.1.A1_at	GRPEL2	-1.0603	0.0000
Ssc.6448.1.S1_at	Q6GMV3	-1.0623	0.0005
Ssc.18204.2.S1_at	CAMTA1	-1.0647	0.0000
Ssc.19203.2.S1_at	CKLFSF4	-1.0654	0.0036
Ssc.13611.1.A1_at	NT5C2L1	-1.0667	0.0014
Ssc.829.1.A1_at	LPIN2	-1.0702	0.0007
Ssc.12335.2.S1_a_at	Q8WVE0	-1.0703	0.0009
Ssc.16577.1.A1_at	ACOX2	-1.0744	0.0113
Ssc.9876.1.A1_at	SNX9	-1.0771	0.0005
Ssc.1210.1.A1_at	C14orf130	-1.0773	0.0000
Ssc.24981.1.S1_at	Q8TE89	-1.0781	0.0001
Ssc.20184.1.S1_at	ARHGEF12	-1.0800	0.0001
Ssc.10076.1.S1_at	C19orf2	-1.0825	0.0018
Ssc.13929.1.S1_at	BRMS1L	-1.0862	0.0001
Ssc.2760.1.A1_at	GNG12	-1.0878	0.0000
Ssc.26779.1.A1_at	CDH17	-1.0915	0.0011
Ssc.29650.1.A1_at	CHEK1	-1.0916	0.0051
Ssc.6790.1.A1_at	Q9H2X4	-1.0916	0.0001
Ssc.25151.1.S1_at	C6orf79	-1.0983	0.0002
Ssc.4306.1.A1_at	MESDC1	-1.0984	0.0001
Ssc.9606.1.A1_at	OPHN1	-1.0999	0.0035
Ssc.24353.2.S1_at	VRK1	-1.1015	0.0181
Ssc.16873.1.S1_at	WDR44	-1.1031	0.0011
Ssc.11164.2.S1_a_at	Q96JN1	-1.1034	0.0331
Ssc.12925.1.A1_at	TXNDC7	-1.1037	0.0000
Ssc.2503.1.S1_at	B3GNT6	-1.1037	0.0001
Ssc.25535.1.S1_at	TM6SF1	-1.1059	0.0010

Ssc.29579.1.A1_at	PDE8A	-1.1079	0.0031
Ssc.14573.1.S1_at	EYA2	-1.1091	0.0005
Ssc.21185.1.S1_at	Q9P092	-1.1106	0.0045
Ssc.30491.1.A1_at	GCSH	-1.1116	0.0017
Ssc.18568.1.A1_at	SCUBE1	-1.1121	0.0003
Ssc.15609.1.S1_at	EGLN2	-1.1161	0.0003
Ssc.8547.1.A1_at	BRIP1	-1.1170	0.0000
Ssc.30090.1.A1_at	AKT3	-1.1196	0.0000
Ssc.28912.1.S1_at	TMEM15	-1.1219	0.0000
Ssc.31023.1.A1_at	RWDD3	-1.1220	0.0006
Ssc.4857.2.S1_a_at	PXMP2	-1.1228	0.0003
Ssc.1379.1.S1_at	Q8N9G7	-1.1239	0.0108
Ssc.20772.1.S1_at	USP39	-1.1275	0.0005
Ssc.6323.1.S1_at	ADFP	-1.1291	0.0001
Ssc.10341.1.S1_at	HELZ	-1.1305	0.0000
Ssc.4713.1.S1_a_at	DHPS	-1.1312	0.0000
Ssc.8254.1.A1_at	KCY_HUMAN	-1.1315	0.0000
Ssc.2243.1.S1_at	C20orf72	-1.1318	0.0001
Ssc.21840.1.S1_at	NUDT5	-1.1322	0.0000
Ssc.19928.1.S1_a_at	DUT	-1.1324	0.0018
Ssc.6338.2.S1_at	USP1	-1.1354	0.0054
Ssc.30633.1.S1_at	NP_060835	-1.1368	0.0011
Ssc.5517.1.A1_at	MAP3K12	-1.1378	0.0021
Ssc.17843.1.A1_at	ANKRD32	-1.1402	0.0018
Ssc.27374.1.A1_at	RFC5	-1.1408	0.0001
Ssc.923.1.A1_at	METAP2	-1.1408	0.0001
Ssc.19675.1.S1_at	RACGAP1	-1.1424	0.0101
Ssc.17833.2.S1_at	SS18L1	-1.1439	0.0005
Ssc.9498.1.S1_at	TAX1BP3	-1.1453	0.0000
Ssc.30818.1.S1_at	NUFIP1	-1.1461	0.0005
Ssc.8163.1.A1_at	C6orf74	-1.1475	0.0027
Ssc.30340.1.A1_at	RPGR	-1.1477	0.0002
Ssc.8009.1.A1_at	LRP1B	-1.1493	0.0000
Ssc.6623.1.S1_at	NIPSNAP3A	-1.1520	0.0045
Ssc.14221.1.S1_at	CPSF5	-1.1524	0.0019
Ssc.5102.1.S1_at	MRPS27	-1.1525	0.0001
Ssc.30936.1.S1_at	ACTR8	-1.1551	0.0009
Ssc.30856.1.A1_s_at	JMJD1A	-1.1552	0.0017
Ssc.8554.2.S1_at	MRPL18	-1.1555	0.0004

APPENDIX – III (B)

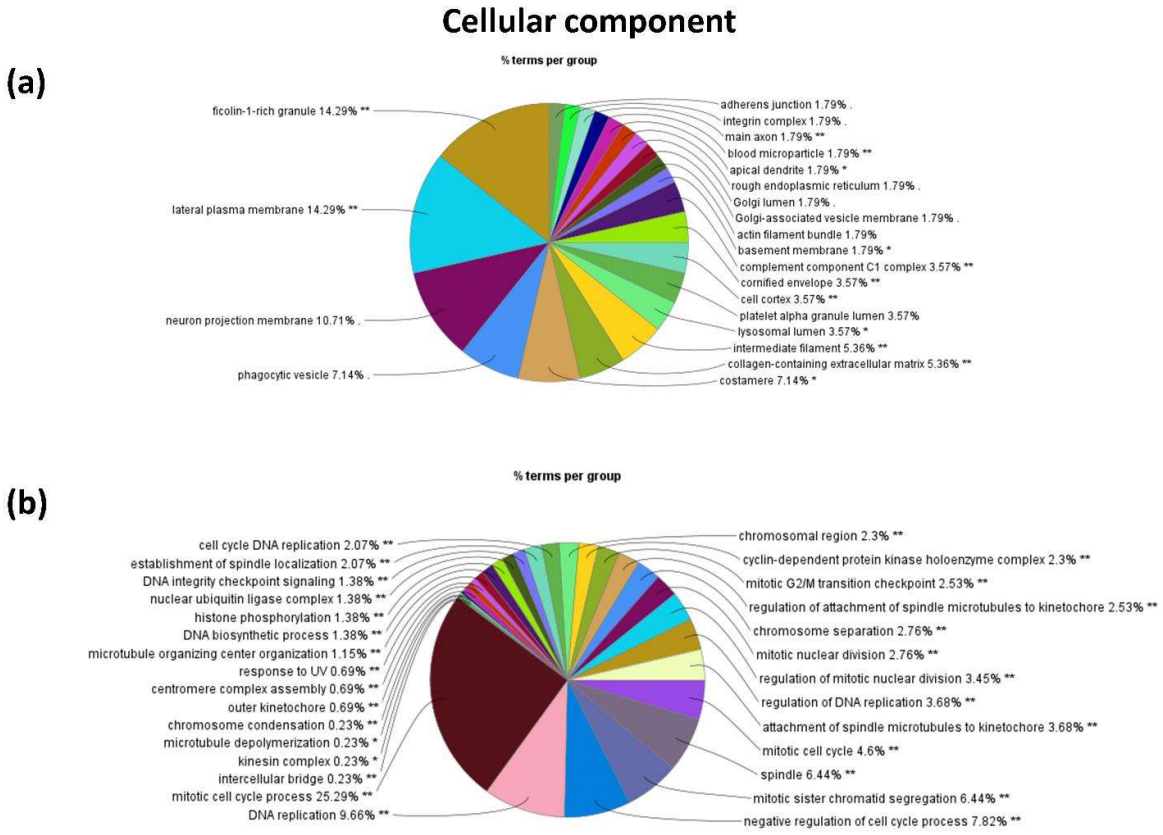

Figure A.1 Cellular component (CC) of enrichment analysis: (a) Upregulated genes; (b) Downregulated genes.

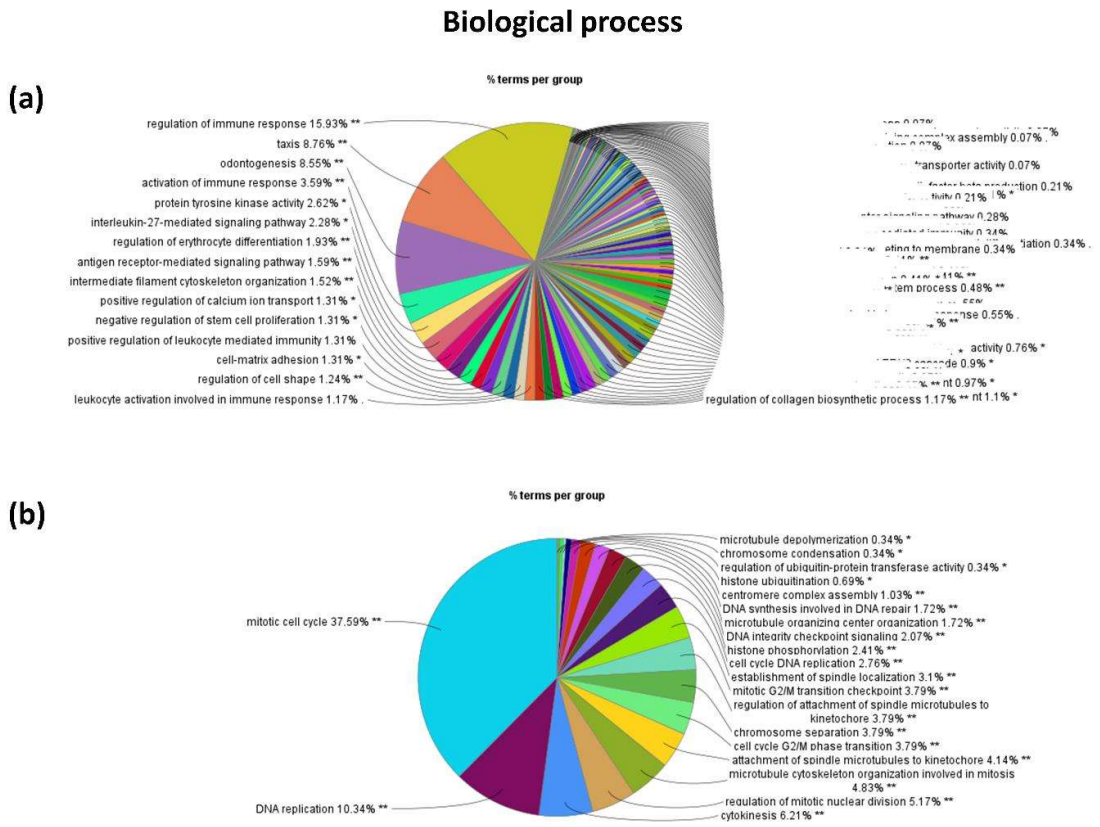

Figure A.2 Biological process (BP) of enrichment analysis: (a) Upregulated genes; (b) Downregulated genes.

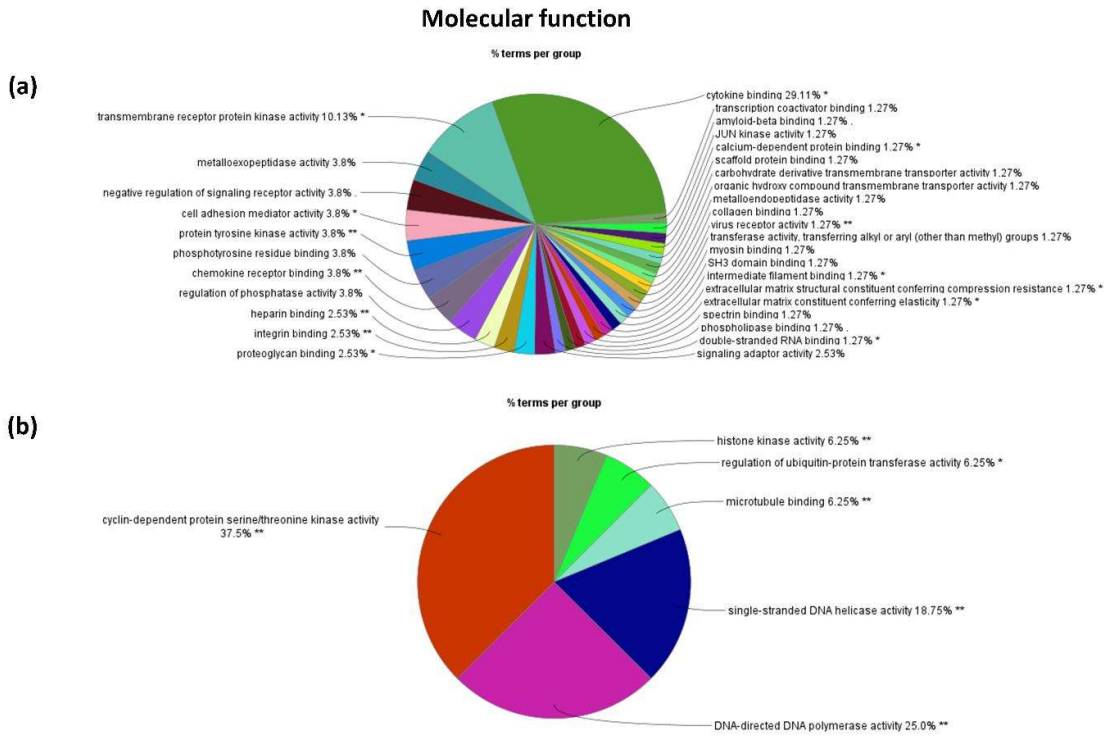

Figure A.3 Molecular function (MF) of enrichment analysis: (a) Upregulated genes; (b) Downregulated genes

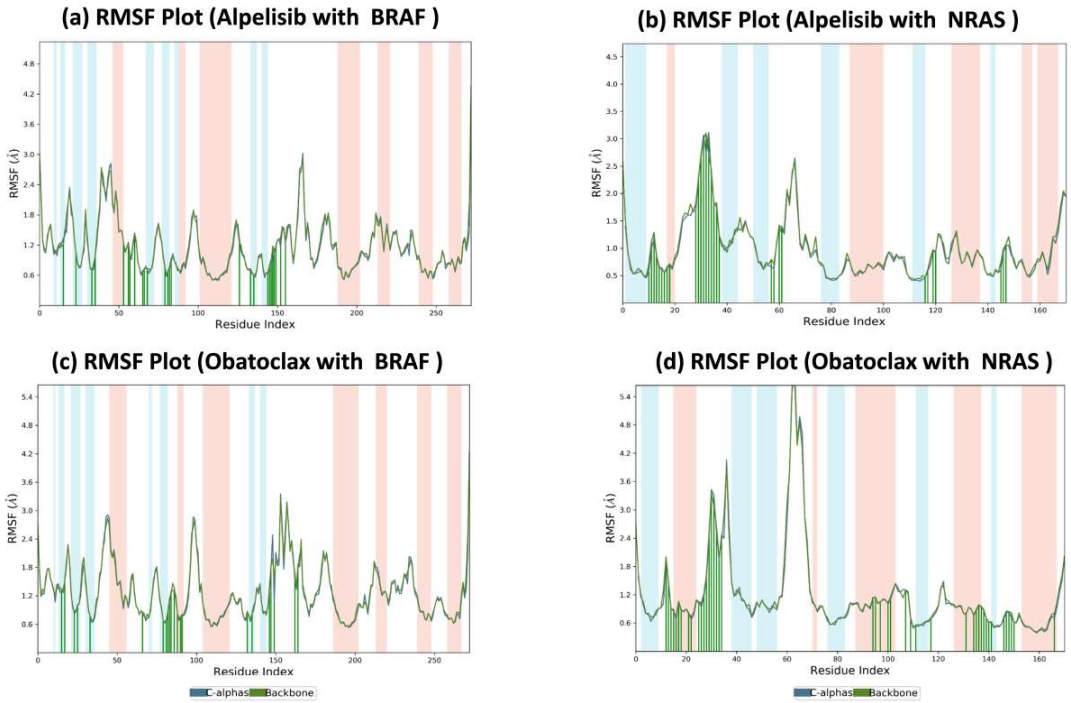

Figure A.4 Molecular Dynamics (MD) simulation trajectories analysis of both BRAF (PDB ID: 5C9C) and NRAS (PDB ID: 6ZIZ) with both the ligand (Alpelisib and Obatoclax). Panel (a, b, c, and d) illustrate the RMSF plot showing how the protein chain's alpha helixes (red color) and beta sheets (blue color) distributions, as well as local fluctuations, changes during the course of the simulation. Green bars represent the ligand interaction locations with the particular residues.

LIST OF PUBLICATIONS

Journals related to the thesis work:

1. **Kumari B,** Sakode C, Lakshminarayanan R, Roy PK. Computational systems biology approach for permanent tumour elimination and normal tissue protection using negative biasing: Experimental validation in malignant melanoma as case study. Mathematical Bioscience and Engineering. 2023 Mar 21;**20**(5):9572-9606. doi: 10.3934/mbe.2023420. PMID: 37161256.

2. **Kumari, B**., Sakode, C., Raghavendran, L., Purohit, P., Bhattacharjee, A., & Roy, P. K. (2022). A Mechanistic Analysis of Spontaneous Cancer Remission Phenomenon: Identification of Genomic Basis and Effector Biomolecules for Therapeutic Applicability, (3 Biotech Journal), **13**(113), DOI-10.1007/s13205-023-03515-0

3. **Kumari, B.**, Arushi, M., Ashish S., Ashutosh, S., & Roy, P. K., Spontaneous cancer regression as reversion of spontaneous cancer progression: Molecular targets and pharmacological implications, (Journal of Bimolecular Structure and Dynamics) (under communication)

LIST OF PUBLICATIONS

Conference publication related to the thesis work:

1. **Kumari, B**., Sakode, C., Raghavendran, L., & Roy, P. K., System biology approach to normal tissue protection in cytotoxic cancer therapy: Experimentally validated gene/signaling basis – melanoma as case study., Annals of Oncology (2022) 33 (suppl_7): S356-S409. 10.1016/annonc/annonc1059
2. **Kumari, B**., Sakode, C., Raghavendran, L., & Roy, P. K., Systems biology basis of permanent tumour regression with normal tissue protection: Experimentally validated signaling pathway framework. J. Clinical Oncology, 40 (16), Supp.1, e15066, 2022 https://ascopubs.org/doi/10.1200/JCO.2022.40.16_suppl.e15066
3. **Kumari, B**., Sakode, C., & Roy, P. K., "Experimentally Validated Systems Biology-Based Approach Enables: (1) Permanent Tumour Remission, With (2) Normal Tissue Protection" Proc. International Conference on Role of Immune System for Cancer Prevention and Treatment. *Annual Conference, Society of Translational Cancer Research*, 2020
4. **Kumari. B.,** Roy, P.K., (2023) "Genomics Basis and Nodal Genes of Endogenous Spontaneous Cancer Remission Phenomenon: Network Pharmacology and Biosystems Analysis.", 42nd Annual Conference of the IACR (Indian Association of Cancer Research), ACTREC at Tata Memorial Center, 2023.

LIST OF PUBLICATIONS

Publications not related to the thesis work:

1. Prakash, A., **Kumari, B.,** & Sharma, S. (2019). A low-cost, wearable sEMG sensor for upper limb prosthetic application. Journal of medical engineering & technology, 43(4), 235-247.

2. Ruttala, R., Purohit, P., Bhattacharjee, A., **Kumari, B.,** & Roy, P. K., (2022). MRI-DTI Imaging Reveals Specific Neuro-degeneration Signature in Precuneus Node of Awareness Processing in Brain under Alzheimer's Disease. Journal of Advanced Applied Scientific Research, **4**(4), 102-111.

3. Chowdhury S, Purohit P, Bhattacharjee A, **Kumari B**, Roy PK, "Novel Drug Discovery for Acute Encephalitis using A.I.-based machine-reading and knowledge-mapping of Medical Literature Text", Proc. NAMSCON 2021.

4. Baghel B, **Kumari B**, Bhattacharjee A, Purohit P, Roy PK, "Long-term Structural Stability observed in Cerebellum during Ageing: Radiological Genomics identifies Neuroprotective Drugs with Clinical Validation", Proc. NAMSCON 2021

5. Kumari, B, Prakash, A, Sharma, S. Development of EMG Sensor for Prosthetic Hand Control, International Conference on Innovation Research in Applied physics, Material sciences, Instrumentation, Electronics, Communication, Electrical, Power Control, Computer system, and Information technology at Jawaharlal Nehru University(TECHNOVA-2017), New Delhi.

Patent:

Prakash, **B. Kumari**, S. Sharma & N. Sharma "EMG sensor for prosthetic hand control," Indian Patent Ref. No. 201811016601, May 2, 2018 (status: published).

International Conferences:

1. **Kumari. B.,** Roy, P.K., (2023) "Genomics Basis and Nodal Genes of Endogenous Spontaneous Cancer Remission Phenomenon: Network Pharmacology and Biosystems Analysis.", 42nd Annual Conference of the IACR (Indian Association of Cancer Research), scheduled on January. 12-16, 2023, ACTREC at Tata Memorial Center, Navi Mumbai, India.
2. **Kumari. B.,** Sakode, C., Lakshminarayanan, R., Roy, P.K., (2022) "Systems Biology approach to Normal Tissue Protection in cytotoxic Cancer Therapy: Experimentally-validated gene/Signalling basis-Melanoma as a case study-.", ESMO (European Society for Medical Oncology) Congress-2022, 9-13 Sept, Paris, France.
3. **Kumari. B.,** Sakode, C., Roy, P.K., (2020) "Experimentally-validated Systems Biology-based approach to enabling Permanent Tumour Remission with Normal Tissue protection-.", 8th International Translational Cancer Research Conference on 'Role of Inflammation and Immune System for Cancer Prevention and Treatment', Dept. of Biochemistry, Institute of Science (BHU) and Society for Translational Cancer Research(STCR), Feb. 13-16, 2020, BHU, Varanasi.
4. **Kumari. B.,** Prakash, A., Sharma, S., (2023) "Development of Neuromuscular EMG Acquisition and Processing for Neural Control of 3-D printed Prosthetic Hand.", 15th meeting of Asian-Pacific society of Neurochemistry (APSN)- 2018, MACAU S.A.R, China,2018.

5. **Kumari. B.,** Prakash, A., Roy, P.K., (2023) "Development of EMG sensor for Prosthetic Hand Control.", 36th Annual Meeting of Indian Academy of Neurosciences being held at Banaras Hindu University during 29-31 October 2018.
6. **Kumari. B.,** and, Roy, P.K., 3rd IBRO/APRC Chandigarh Associate Neuroscience School, 2018.
7. **Kumari. B.,** Prakash, A., and Shram., S., "Development of EMG Sensor for Prosthetic Hand Control" TECHNOVA-2017(International Conference) organized by" krishi Sanskrit" at Jawaharlal Nehru University, New Delhi.

Workshops and Hands-on-trainings:

1. **Workshop on Solidworks for Biomedical Applications,** Department of Biomedical Engineering University College of Engineering(A), **Osmania University**, February, 2022.
2. **Workshop on Insilco Drug Designing using Network Pharmacology Approach,** Department of Applied Science, **IIIT Allahabad**, 2021.
3. **Short-Term Course (with Hands-On-Training) on 'Advances in Medical imaging'**, in I-DAPT HUB Foundation, **IIT BHU**, March 2021.
4. An **online short-term certificate course on Analytical Techniques to Study from Biomolecules to Tissues** (ATSBT- 2021), July, 2021
5. **3rd Workshop on 'Brain, Computation and Learning'** at Indian Institute of Science **(IISC) Bengaluru**, INDIA, June 2019.
6. **ISN-APSN Neuroscience School at Macau University of Science and Technology (Macau, CHINA)** in 2018.